



ARL-TR-8333 • APR 2018



The Philosophy, Theoretical Bases, and Implementation of the AHAAH Model for Evaluation of Hazard from Exposure to Intense Sounds

by G Richard Price and Joel T Kalb

Approved for public release; distribution is unlimited.

NOTICES

Disclaimers

The findings in this report are not to be construed as an official Department of the Army position unless so designated by other authorized documents.

Citation of manufacturer's or trade names does not constitute an official endorsement or approval of the use thereof.

Destroy this report when it is no longer needed. Do not return it to the originator.



The Philosophy, Theoretical Bases, and Implementation of the AHAAH Model for Evaluation of Hazard from Exposure to Intense Sounds

by G Richard Price
ALTUS Engineering, Darlington, MD

Joel T Kalb
Human Research and Engineering Directorate, ARL

REPORT DOCUMENTATION PAGE				Form Approved OMB No. 0704-0188	
<p>Public reporting burden for this collection of information is estimated to average 1 hour per response, including the time for reviewing instructions, searching existing data sources, gathering and maintaining the data needed, and completing and reviewing the collection information. Send comments regarding this burden estimate or any other aspect of this collection of information, including suggestions for reducing the burden, to Department of Defense, Washington Headquarters Services, Directorate for Information Operations and Reports (0704-0188), 1215 Jefferson Davis Highway, Suite 1204, Arlington, VA 22202-4302. Respondents should be aware that notwithstanding any other provision of law, no person shall be subject to any penalty for failing to comply with a collection of information if it does not display a currently valid OMB control number.</p> <p>PLEASE DO NOT RETURN YOUR FORM TO THE ABOVE ADDRESS.</p>					
1. REPORT DATE (DD-MM-YYYY) April 2018		2. REPORT TYPE Technical Report		3. DATES COVERED (From - To) 1 January 2016–1 March 2017	
4. TITLE AND SUBTITLE The Philosophy, Theoretical Bases, and Implementation of the AHAAH Model for Evaluation of Hazard from Exposure to Intense Sounds				5a. CONTRACT NUMBER	
				5b. GRANT NUMBER	
				5c. PROGRAM ELEMENT NUMBER	
6. AUTHOR(S) G Richard Price and Joel T Kalb				5d. PROJECT NUMBER	
				5e. TASK NUMBER	
				5f. WORK UNIT NUMBER	
7. PERFORMING ORGANIZATION NAME(S) AND ADDRESS(ES) US Army Research Laboratory ATTN: RDRL-HRF-C Aberdeen Proving Ground, MD 21005				8. PERFORMING ORGANIZATION REPORT NUMBER ARL-TR-8333	
9. SPONSORING/MONITORING AGENCY NAME(S) AND ADDRESS(ES)				10. SPONSOR/MONITOR'S ACRONYM(S)	
				11. SPONSOR/MONITOR'S REPORT NUMBER(S)	
12. DISTRIBUTION/AVAILABILITY STATEMENT Approved for public release; distribution is unlimited.					
13. SUPPLEMENTARY NOTES					
14. ABSTRACT The Army has adopted the Auditory Hazard Assessment Algorithm for Humans (AHAAH) as the method of assessing impulsive noise hazards in the MIL-STD 1474 Military Noise Standard (2015). AHAAH is a physiological-dynamics-based advance over nonphysical, wholly empirical, external energy-damage correlation methods for evaluating hearing damage risk associated with impulsive noise exposure. AHAAH applies the physical auditory dynamics of the external, middle, and inner ear, to biomechanically model the ear's response to impulsive sound and determine the strain-induced damage occurring in the cochlea's organ of Corti. AHAAH's physical dynamics includes observed nonlinear behavior in the middle ear. AHAAH is validated against the measured results of human exposures to impulsive sounds, and unlike wholly empirical correlation approaches, AHAAH's physical basis gives it improved applicability in estimating the auditory risk caused by impulses not previously considered. The Hearing Protection Module of AHAAH allows the evaluation of hearing damage risk for persons using hearing protection when exposed to impulsive noise. The module includes nonlinear hearing protectors as well as many linear protectors. Research and development supporting the creation of AHAAH are described, along with potential approaches for continued improvements in AHAAH and in the assessment of auditory hazards associated with impulsive noise exposure.					
15. SUBJECT TERMS impulse, auditory hazard, damage risk, assessment, electroacoustic analogy, noise standard					
16. SECURITY CLASSIFICATION OF:			17. LIMITATION OF ABSTRACT UU	18. NUMBER OF PAGES 90	19a. NAME OF RESPONSIBLE PERSON Dr Paul D Fedele
a. REPORT Unclassified	b. ABSTRACT Unclassified	c. THIS PAGE Unclassified			19b. TELEPHONE NUMBER (Include area code) (410) 278-5984

Contents

List of Figures	v
List of Tables	vi
1. Introduction	1
2. Hearing Science and the AHA AH Model	2
2.1 Historical Context	4
2.2 A New Approach to Hazard Assessment: The AHA AH Model	6
2.3 Unique Features	8
2.4 Commitment to the Physiological Model and Its Interpretation	9
2.5 Limits on the Interpretation of the AHA AH Model	10
3. Development of the Model: Insights from Basic Research	11
4. Basic Modeling Considerations	13
4.1 Contributions of the Middle Ear	15
4.2 Middle Ear Muscle Effects	18
5. The Model in Quantitative Detail	22
5.1 The Conductive Path	22
5.2 Cochlear Susceptibility	23
5.3 Opportunities to Adjust the Model	28
5.4 Stapes to BM Transfer Functions	30
5.5 Confronting the Model with Data and Adjusting It	31
5.6 Accounting for Individual Differences in Susceptibility	32
5.7 Creation of the Human Model	35
5.8 Additional Features of the Model	37
5.9 “Hidden Features”	39
5.10 Dealing with Protected Hearing	41

5.11	HPD Performance Measures	43
5.12	The Hearing Protection Module (HPM)	44
6.	The Problem of Which Standard to Apply for Protected Ears	47
6.1	Mathematical Aspects of the AHAAH Model	47
6.2	Stepping Through the Program Calculation	53
6.3	Parameter Values and Differential Equations	55
7.	Conclusion	65
8.	References	66
	Appendix A. Physical Constant Definitions	75
	Appendix B. Computer Programming and Source Code Applications	79
	List of Symbols, Abbreviations, and Acronyms	80
	Distribution List	81

List of Figures

Fig. 1	Anatomical and circuit diagrams of the ear and its electroacoustic analog. The loops indicate paths through which current flows.	1
Fig. 2	Cross-sectional view of the cochlea showing the orientation of the BM and the organ of Corti resting on it	14
Fig. 3	Diagram showing location of tip links at top of hair cells	14
Fig. 4	Attenuation produced by the middle ear muscle contraction in the AHA AH model	21
Fig. 5	Transfer functions in the AHA AH model for stapes displacements to basilar membrane displacements for pure tone stimuli.....	30
Fig. 6	CTS for 12 experiments with the cat ear (see text) exposed to impulsive sounds as a function of the auditory risk units (ARUs) calculated with the AHA AH model of the cat ear. Each data point represents the mean loss at the frequency showing greatest loss for both ears of 10 cats. The trend line represents the least squares fit to all the data.	32
Fig. 7	Transfer function for free-field pressure to pressure at eardrum. Magnitude appears in the upper panel and phase in the lower panel. The dots are data (Mehrgardt and Mellert 1977) and the lines are the calculation by the model.	35
Fig. 8	Transfer function for eardrum pressure to stapes volume velocity. Magnitude appears in the upper panel and phase in the lower panel. The dots are data and the lines are the calculation by the model. Transfer function data from Kringlebotn and Gunderson (1985).	36
Fig. 9	Circuit diagram of the 3-piston model of a hearing protective device	45
Fig. 10	Diagram of AHA AH, an electroacoustic analog of the ear	48
Fig. 11	Transfer function for free-field pressure to pressure at eardrum. Magnitude appears in the upper panel and phase in the lower panel. The dots are data (Mehrgardt and Mellert 1977) and the lines are the calculation by the model.	50
Fig. 12	Transfer function for eardrum pressure to stapes volume velocity. Magnitude appears in the upper panel and phase in the lower panel. The dots are data and the lines are the calculation by the model. Transfer function data from Kringlebotn and Gunderson (1985).	51
Fig. 13	The ladder network, corresponding ear sections, and in each section, the currents, in dynamically equivalent to volume velocities in the ear	56
Fig. 14	Details of volume element representation in ear canal	61
Fig. 15	Annular ligament shown as one of N standard springs.....	63

List of Tables

Table 1	List of definitions and default values for all AHAAH calculation coefficients included in the file "man.coe"	57
---------	--	----

1. Introduction

The Auditory Hazard Assessment Algorithm for Humans (AHA AH) has moved from basic science to practical use in predicting hazards to the human ear from exposure to intense sounds, typical of gunfire (MIL-STD-1474E). As a noise standard it is unique in many ways. In the past, standards have been expressed as a simple line on a graph (MIL-STD-1474D, for example) or in a measured level (L_{AEQ8} of 85 dB). The approach in MIL-STD-1474E is very different. Previous standards tried to find a correlation between some standard measure of sound pressure and hearing loss; but in the case of AHA AH, the approach was to first understand the physiological processes underlying hearing loss and then find a measure that predicts it. In the final analysis, it is an implementation of an electroacoustic model of the ear—the AHA AH—that is embodied in a computer program. The circuit diagram of the electroacoustic model is shown in Fig. 1. The user provides digitized pressure histories of acoustic impulses and the model calculates the hazard resulting from the exposure.

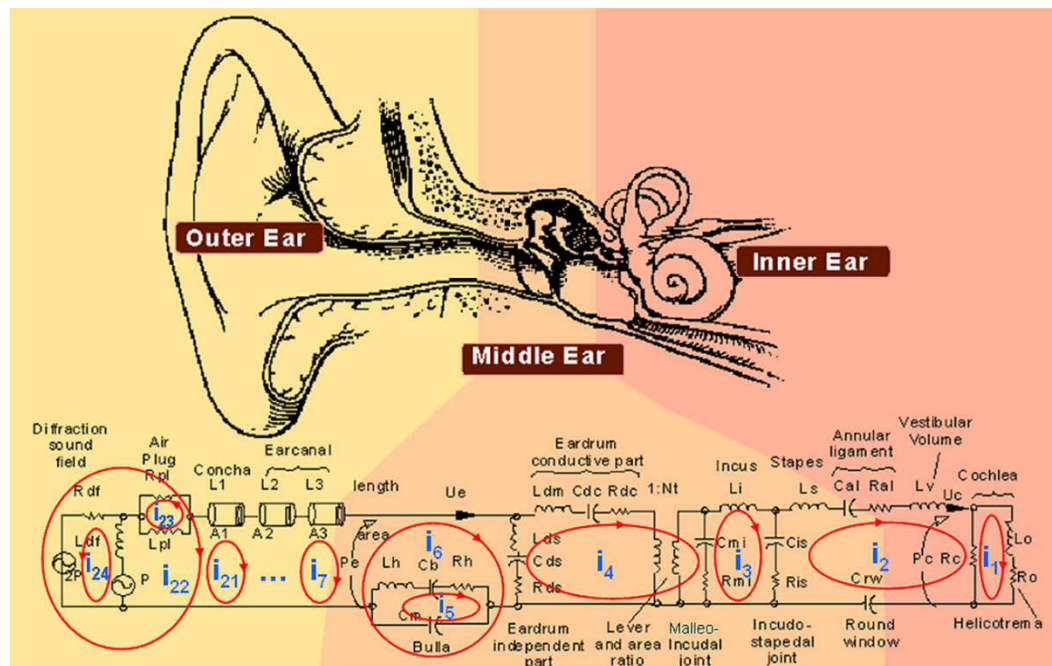


Fig. 1 Anatomical and circuit diagrams of the ear and its electroacoustic analog. The loops indicate paths through which current flows.

In the long term, it is important that the model remain applicable to military situations, and the algorithms within the model remain calculable no matter how future computer operating systems and programming languages may change. In order to ensure that in the future it (and any amended successor) remains compatible with the practices and the then-current computational system(s), we write this

report to make explicit the basic assumptions and philosophy determining the approaches used in forming the model, and further, to document the scientific data supporting the variables within the model. Knowing *why* some particular construction is used may be as useful as documenting the choice of a specific value or calculational procedure. Hopefully, these thoughts will assist those involved in a configuration management program in carrying out their responsibilities while retaining or improving the model's scientific validity. Recent experience has shown the need for such a document as this. A paper by Zagadou et al. (2016) was critical of the AHAAH model, and proposed changes. We reviewed the paper (Price et al. 2017a, 2017b) and found it to be seriously flawed in many aspects. A discussion, such as the present one, might have promoted a better outcome.

To that end, we produced this report aimed at specific audiences: 1) the administrator or hearing scientist concerned with the scientific issues behind the AHAAH model, 2) the programmer or scientist associated with the details regarding the choice and use of the variables in the AHAAH model, and 3) the programmer concerned with the algorithms used in the model's calculations. Taken together, we believe that we addressed most of the issues that might arise in maintaining the AHAAH model as a standard.

2. Hearing Science and the AHAAH Model

In this section, we will attempt to provide a unifying conceptual context for hazard evaluation, which includes brief comments on the contrasts between the new method and existing methods of hazard analysis. Discussion will reference the literature involved in the development and validation of the AHAAH model, rather than reproduce it. We will focus on both the science and the philosophy underlying critical elements of the ear's physiology that must be accommodated for accurate predictions. These are non-arbitrary issues that must be accounted for. We will also cover the basis for the model's design and the implications for its use, comparing and contrasting it with alternate procedures. In addition, we will address its validation and the issues associated with the available data sets usable in evaluating a damage risk criterion (DRC) for intense sounds.

The problem of a “conservative bias” in standard development. From the standpoint of the hearing conservationist, the primary focus of a noise standard is protecting Warfighters from developing hearing loss associated with noise exposure. Such noise exposures must be limited on humanitarian grounds and, alternatively, in the national interest, limits are essential to preserving an effective fighting force. A conservative approach of this sort is clearly justified and has been the motivating force behind health hazard assessments for weapons noise.

An alternate viewpoint applies as well. This noise standard is designed for use in a military setting, to include the design and use of weapons. From a tactical standpoint, more effective weapons—typically more powerful weapons—are an asset. Increased power and range save our Soldiers' lives. However, more power tends to be accompanied by increased noise. A 3-dB change in pressure (not a large change in the world of hearing conservation) reflects a 50% change in energy—a massive change where weapons performance is concerned. From the operational perspective, preservation of life is greatly enhanced by attacking from outside the range of the enemy's weapons—conservatism of another sort. Reducing sound exposures just to protect hearing is not acceptable. A good answer must include mission success, as well as preserving both lives and hearing.

Requirements for and effects of hearing protection devices (HPDs). The sound fields associated with virtually all impulse-producing weapons are potentially hazardous and hearing protection should be worn. However, HPDs increase the complexity of dealing with the hazard. There is little doubt that a properly fitted and worn HPD will protect the ear from almost all exposures. That is the good news.

The secondary effect of the HPD is that its attenuation will effectively reduce the wearer's sensitivity to all sounds. This results in a loss of auditory situation awareness (especially critical for the infantry), as well as in a greatly reduced ability to understand speech. The seriousness of this loss in a military setting has only recently come to be appreciated (Sheffield et al. 2016). For example, in a quiet setting, with a good ear, one can hear an individual walking in leaves about 100 m away (Price et al. 1989). This implies that a sentry would have about 2-min warning that someone was approaching. But with a relatively small hearing loss, the sentry has no warning—a life-threatening situation in combat.

In another context, research on the effect of speech intelligibility on military performance suggests that there is a 1:1 correspondence between speech intelligibility and mission success (at least for armored operations) (Peters and Garinther 1990). A change in speech intelligibility could be brought about by a variety of factors, such as the quality of the communication system or the Soldier's ability to hear. Thus, a 20% change in speech intelligibility resulted in a 20% change in *mission success*. There is little we could do to a tank—increase weapon accuracy, reduce fuel consumption, etc.—that could have such a large effect. Good hearing is essential to effective military performance.

The combat Soldier faces a particular problem—do not wear hearing protection and lose your hearing (and your effectiveness as a Soldier), or wear hearing protection and reduce your hearing sensitivity. This “damned-if-you-do and damned-if-you-

don't" dilemma has resulted in the development of HPDs that are nonlinear (i.e., they attenuate little at lower sound pressure levels [SPLs], where the Soldier needs to hear); but their attenuation increases as the level rises (where the Soldier needs protection). As we will see later, describing the performance of these HPDs remains something of a challenge.

Thus there is no "safe error" to make in the interests of conservatism. Both over-restrictive standards and under-restrictive standards must be avoided. An appropriate standard needs to be an accurate reflection of the true state of affairs. The organization must then determine just what risks must be taken.

2.1 Historical Context

For the American military, the problem of predicting and ameliorating the effect of very intense sounds on hearing can be traced to our experience in World War II. Our knowledge began to grow very slowly. Given the primitive state of acoustic instrumentation in those years, the inherent difficulty of working at very high SPLs, the very limited knowledge of the ear's behavior at high intensities, as well as a lack of official interest in producing funding for science, research in the early years was understandably sporadic and largely descriptive. Nevertheless, given the need for some method of assessing hazard, by the 1960s and 1970s several attempts had been made to relate some parameters of the measured sound to potential hazards for the human ear. In the US and the UK an approach based on the work of Coles, Garinther, Hodge, and Rice (1967, 1968) was the basis for MIL-STD-1474; the Netherlands had the Smoorenburg criterion (Smoorenburg 1982); and Germany had the Pfander criterion (1975). They all had been developed primarily with evidence from small arms exposures, depended on measures of peak pressure and differing measures of duration, and were essentially linear. In no case did they take specific account of the acoustic or physiological characteristics of the ear. They focused on finding a measure of the sound, which could be reliably made, and empirically relating it to hearing loss by correlational techniques. The ear was treated as a "black box" and higher sound pressures and longer durations—variously defined—were associated with greater hazard. By the 1980s it had become apparent that the existing standards did not work, especially for large-caliber weapons impulses, where they overpredicted hazard. A new method of hazard evaluation was clearly needed.

In the same vein, A-weighted energy had been proposed as a measure that could be correlated with hazard. Insofar as the A-weighting function is derived from measurements of the loudness of a sound, it does begin to open the black box of the ear and reflects the characteristics of the conductive path. It has the advantage of

being relatively easily measured and is now widely used in the evaluation of noise hazard from common industrial sources (sound pressures from 80–85 dB up to 110–115 dB). It has been considered by some as a measure up to the very highest levels (185+ dBP). However, research has shown that an A-weighted level that is tolerable for rifles differs from the tolerable level for cannons by 20–25 dB (Murphy et al. 2009; Price 2007)—with energy from cannons being *more* tolerable. In any event, as we shall see, all these approaches lack the theoretical base needed to address the true complexity of the ear's response to intense sounds at the level of gunfire (145–185+dBP).

An important side-issue with respect to the use of A-weighting for rating hazard relates to the nature of the loss mechanism being modeled as the pressures rise from 85 to 185 dB. Some have argued in favor of the use of an energy measure over the entire range (Murphy and Kardous 2012). However, the data on loss argue in the strongest terms that such a procedure is irrational. One of the arguments in favor of the use of A-weighted energy as a criterion measure over the full range of pressures is convenience—it would allow the evaluation of combined exposures to both intense impulses and continuous noises at much lower levels (a common combination). It is true that it is physically possible to make such a measure and it would, indeed, be convenient if it were valid.

However, the ultimate question is whether or not it is rational to do so. The essential problem is that it has long been established that the loss mechanisms operative in the ear change as the level rises. At lower levels common in industrial settings (85–100 dB), the losses accumulate as a function of the logarithm of the exposure time and will recover within 16 h or so. Such exposures can be repeated daily for many years and permanent losses grow slowly. For such exposures, databases such as those in ISO-1999 and ANSI S3.44 can be used to estimate the threshold shifts from such exposures. At the physiological level, the loss mechanism is conceived as metabolic exhaustion—the ear is tired out. At higher levels (above about 140 dB) things change dramatically (Price 1981). The losses accumulate in linear time, recoveries are extended and may not run to completion, and permanent hearing loss can occur from one exposure. At the physiological level, the damage mechanism has changed to one of cellular disruption; the ear is being “torn up” not “tired out”. It is obvious that if these things are true, no matter how convenient it would be to calculate a single energy measure, lower level and higher level exposures simply cannot be treated as equivalent. In fact, the AHAH model, which will be described next, was developed specifically to deal with losses at levels above 140 dBP.

2.2 A New Approach to Hazard Assessment: The AHAAH Model

In contrast to the previous approaches, the AHAAH was developed from a theoretical perspective—if we first understand the damage processes at work in the ear, a predictive metric could be devised. The decision to work using a first-principles approach was made deliberately, recognizing that it involved great technical complexity and that such an approach had not been used before in the development of a DRC. However, the important advantages of such an approach—should it succeed—resulted in the decision to make the model an electroacoustic analog of the ear that is conformal with the structure of the ear. Each point is worth examining.

Electroacoustic models have been used successfully in describing dynamic systems, such as loudspeakers. Arguably, the ear is like a loudspeaker being driven in reverse. Therefore, electroacoustic descriptions of the ear's behavior are mathematically tractable and commonly used because they reflect the integrated behavior of a system. The use of such tools has much to recommend it.

The second consideration was to try to maintain parallelism between the anatomical structure of the ear and the elements in the model. Generally speaking, scientists argue that for efficiency and simplicity's sake, it is wise to keep the number of variables in a theory to a minimum. In that spirit, it would have been possible to conceive of the external and middle ears as a band-pass filter conducting best in the 2–4 kHz region (for the human ear). Such a filter can be described relatively simply. However, to maintain conformality between the model and the ear, we identified the physiological elements involved in acoustical energy transfer from free sound field to the stapes, including head-induced diffraction and reflections within the ear. Inclusion of these elements produced a great deal of additional complexity—in one sense, a disadvantage—but their inclusion produced the capacity to generate engineering insight into the mechanisms at work and the potential for evaluating subtle elements of the ear's response. These elements were translated into a schematic diagram using the electroacoustic analogy (Fig. 1). Regions moving in phase (such as each ossicle) were approximated by a lumped-parameter circuit component. More extended objects, such as the ear canal or the eardrum, were subdivided (i.e., they were divided into sections that are small compared to the highest frequency of interest [hence move in phase] or else are modeled as transmission lines). The result is that the AHAAH model has some 69 variables. In science, simpler may be better in most circumstances, and such a large number of variables may seem daunting. We have found that the results have been worth the effort.

Conformality with the physical structure maximizes the utility of the model as well as provides for the possibility of engineering insight and innovation. For instance, because head-related transfer functions and the ear canal effects are separately calculated, it is possible to evaluate the effects of HPDs applied over the ear or alternatively in the ear canal. If, in the future, an HPD over- or under-pressurized the external ear canal, that effect could be evaluated. The AHAAH model offers innovators maximum flexibility.

Admittedly, having a large number of variables means that there are many opportunities to “get it wrong”. There is, however, a safety net—reality. Fortunately, most of the variables relate to real physical elements whose properties are known or can be reasonably estimated. Heads are only so big, the bones of the middle ear have masses and sizes that are known, the ear canal has a limited range of dimensions, and so forth. Values chosen for such variables have to be anatomically reasonable. That being said, there are situations in which the exact physical size may not be the “best” value. A microphone, for example, may be a half-inch in diameter; but because its diaphragm is rigidly fixed at its circumference, its “effective size” is somewhat smaller. Or the stapes in the human ear moves with a rocking motion, making it a dipole radiator rather than a simple piston. Therefore, its effective size is smaller than its physical size. Such allowances were made in the modeling used here. Our ultimate goal was to have the model match the transfer functions as closely as possible.

We needed to get the transmission transfer functions correct and we could because the transfer functions from the free field to the cochlear entrance—both magnitude and phase—are known. If the model matches these, then we can be confident that it is correctly representing the elements of the conductive path. Getting good agreement between the model and the transfer function(s) was the touchstone in establishing values for the variables. We have already noted that maintaining parallelism between the model’s elements and the ear’s physiology promotes both flexibility and insight. The overwhelming advantages of such an approach have been that it 1) enhances generalizability and 2) enables insights into mechanisms that could be exploited to reduce auditory risk, as well as promotes the design of weapons systems that are both more effective and inherently less hazardous. Consider each of these issues in turn.

Generalizability. As previously noted, most standards have been developed with correlational techniques in which ears were exposed to some given type of impulse and the effect on hearing threshold measured. In such a case, one can use the results to predict confidently (given that within- and between-subject variables are not a problem), so long as any new test impulses or other variables are *exactly* like those used in the original tests. MIL-STD-1474D, for example, was based almost entirely

on unprotected exposures to small-arms fire. The problem is that in practice, new impulses are often very *unlike* those used in the standardization studies and considerable extrapolation is necessary. This is particularly dangerous when it is not clear that there is a meaningful continuum along which impulses are being ranked. For example, the previously existing standards used peak pressure, duration, or energy, which at first blush would appear to relate to hazard. However, experience has shown that there are other variables internal to the ear that are critical in the development of hazard, and as a result the traditional variables tend to fail badly (i.e., energies and durations greatly *over-predict* the hazard from large caliber weapons (Murphy et al. 2009; Price 2007). If, on the other hand, the criterion is theoretically based, the relationship between the measurements and the variable(s) producing hearing loss are more closely related, predictive ability increases, and the risks associated with extrapolation are very much smaller (not every new impulse affects the ear like the “old” ones).

Insight. In addition to generalizability, the theoretical approach offers the potential for meaningful design insight, enabling the creation of less hazardous products, as well as the potential for improved system performance. For example, if we measure the weighted energy in an impulse as is typically done, then we lose the information in the waveform regarding exactly when in the impulse the energy was delivered (we look at only the magnitude of the frequency-domain information and ignore the phases). However, the ear operates in the time domain—it contains displacement-related nonlinearities, which means that exactly *where* things are at a particular moment is important. This gain in analytical power can be critical to the assessment of hazard.

2.3 Unique Features

In addition to making a numeric assessment of hazard, the model does something unique—it makes a “movie” of the evolution of hazard during the analysis period. Thus, for the first time, it is possible to relate specific portions of the waveform to the development of hazard. As we have just argued, for some impulses the exact sequence of events is critical. Calculations with the AHAH model and their realization in experimental data have demonstrated that the exact timing of the peaks and dips in the waveform does matter for particular impulses. For example, in the presence of a peak-clipping nonlinearity produced by the stapes suspension, the timing of peaks and dips in the waveform is important in determining the energy that gets transmitted to the cochlea, the primary damage site. Using this feature of the AHAH model, it has been calculated that exposure to automotive airbag noise should be safer with the windows closed rather than open, even though the pressures are higher (peak clipping during the higher pressure reduces the flow of

energy to the inner ear) (Price 2006a). Happily, Sommer, and Nixon (1973) had found this mechanism explained their otherwise paradoxical results with human subjects (Ss) exposed to the elements of airbag noise. Or, it has been experimentally demonstrated that an impulse from a rifle with a muzzle brake can be no more hazardous than the impulse from a standard weapon (Price 2003), in spite of the 10 dB higher peak pressures and energies associated with the muzzle brake.

If a DRC evaluates only peak pressure, duration, or energy, then the only advice that can be given to the designer is to reduce what was measured—advice, which, if followed, may not actually result in a safer exposure or may have other unacceptable consequences (i.e., reduced peak pressure resulting in greatly reduced range in a weapon system; proximity to an enemy holds its own distinctive hazards). With the theoretical insight that can be provided by an approach using the AHAH model, however, the potential exists for weapons to be designed and deployed in ways that are both safer and more effective.

The advantages of enhanced generalizability and the ability to produce engineering insight commended the theoretically based approach. The additional administrative processes necessary to maintain such an electroacoustic model are manageable and a small price to pay for greatly enhanced accuracy and efficiency in the US Department of Defense's efforts to support the Warfighter in combat.

2.4 Commitment to the Physiological Model and Its Interpretation

All the foregoing points being made, the choice of a model faithful to the ear's physiology brings obligations with it as well. The word "model" is often used rather loosely and many "models" are much less formal than AHAH. For instance, someone may simply propose that the phenomenon being analyzed can be adequately described by a particular mathematical function or other measure (e.g., hazard can be modeled by a response to the A-weighted energy in it). Then if a particular L_{Aeq8} does not fit a particular data set, the "model" can be changed and a level that fits better can be proposed. Statistical fits to data sets are often models of this sort.

If, however, the AHAH model's predictions should not fit the data, the process of resolution is much more complex. Its elements have physical meaning. If the model makes a bad prediction, then the modeler has to figure out what aspect(s) of the modeled ear's structure or operation needs to be changed to produce an accurate prediction—a nontrivial exercise, as *all* the aspects of the ear's performance need to be properly fit at the same time, from the transfer functions to the hearing loss data.

2.5 Limits on the Interpretation of the AHAH Model

As with any theory or evaluative scheme, there are limits to the application of the AHAH model. The restrictions on interpretation of the model's output are rationally based. The formula that relates auditory risk units (ARUs) to hearing loss is empirically established (the formula came from a best fit to the 12 different exposures with the cat ear [see Fig. 5]). It predicts no compound threshold shift (CTS) for 200 ARUs—a reasonable outcome. On the other hand, it also calculates “negative CTS” for less than 200 ARUs (e.g., -79 dB for 10 ARUs). Such interpretations should be eschewed as unreasonable extensions of the model output. Likewise, at the other end of the scale, high numbers of ARUs also have limits to their real meaning. For example, an exposure of 3,000 ARUs predicts a CTS of 73 dB and an eventual permanent threshold shift (PTS) of over 40 dB. Research has shown that a 40-dB PTS implies that there are essentially no outer hair cells left at that site in the cochlea. Therefore, it is meaningless to discuss losses at a particular location involving more than 100% of the available cells. Higher exposures would, of course, affect the inner hair cells, which are normally more resistant to damage and would probably also be associated with outer hair cell loss at more distant locations. Nonetheless, there are upper limits to meaningful interpretation.

It is also true that there are limits to the range of sound pressures that AHAH can reasonably be expected to accommodate. It was originally designed for application to the region of intensity where the loss processes are essentially mechanical in nature—in the 140 dB and upward region. Most of the tests with human Ss have been done with impulses whose peak pressure levels (PPLs) have been in the rifle to rocket range—roughly 155–185 dBp. In that range, AHAH has predicted accurately. It is not clear how much lower in pressure an accurate analysis could still be achieved. In fact, the pressure range from about 110–115 dB to 145 dBp is something of an unknown region where the metabolic loss processes and the mechanical loss processes blend. It is reasonable to suppose that the relationship between exposure and loss might be very complex, indeed. Some data on the cat ear and the cochlear microphonic have demonstrated that in that pressure regime, the timing of rest and exposure sequences can result in half (or double) the loss, depending upon whether or not recovery processes are interrupted (Price 1974, 1976). This area could use much additional research.

3. Development of the Model: Insights from Basic Research

The requirement for animal tests. The research program that has culminated in the AHAAH model involved data from studies that have used both animal and human ears. It is worth spending a few moments to document a few of the philosophical issues associated with integrating the data from more than one species. In the present case, it can be quickly seen that for ethical reasons it was necessary to use animal Ss for some data. We were trying to predict hazard that included tissue damage that would result in permanent hearing loss. To have the assurance that predictions of permanent loss were valid, it was necessary to actually produce such losses; however, it would be unethical to use human ears for such tests. The use of animal subjects thus has the advantage of allowing the full range of exposures and their effects to be observed.

Limitations on data when human Ss are used. In passing, we note that even though auditory damage testing may continue within the confines of animal use regulations, the basic interest is in predicting effects for human ears. And if extrapolation from animal data to predicting human effects is to be supported, *some* human data set is needed that will allow a comparison with the animal data. Obviously, where human ears have been used—as, for example in the US, in the early studies in the 1960s by Hodge and Garinther at the US Army Human Engineering Laboratory, or in the later studies by Johnson, Patterson, and their collaborators in the “Albuquerque Studies”—great care was taken to assure that only the signs of incipient damage were observed. Additionally, we have very limited data for temporary losses over 25 dB or for true permanent losses: the region of exposure in which we have the greatest interest. From a statistical perspective, it means that at the very high SPLs of interest here, the behavior of only a very small number of ears (i.e., the most susceptible) can be observed. For example, in the Albuquerque Studies where more than 200 subjects were tested (in about 2,000 individual exposures), threshold shifts of 15 dB or larger were seen in less than 15% (Johnson 1998; Price 2010b). Thus, with human ears we are faced with predicting on the basis of the upper percentiles of susceptibility—a small and an inherently uncertain group. When ears show no loss, that may be interesting data—the exposure was “safe”—but we have no way of knowing just *how* safe the exposure was and, as a result, such data have limited utility in validating a damage model.

Use of animal data. How might we use data from animal ears to predict for the human ear? Often, analysts use no rigorous method in making comparisons; ears are assumed to be generally alike. Yet such assumptions are potentially conflicted. For example, the chinchilla ear and the human ear have almost exactly the same

threshold sensitivity (Miller 1970). This similarity would seem to recommend the chinchilla as a direct-replacement model for the human ear in noise tests. Such an assumption has proved to be untenable. For some reason, as yet unidentified, despite having the same basic sensitivity, the chinchilla ear is much more susceptible to loss than the human ear.

In contrast, our approach was aimed at making the fewest assumptions regarding the correspondence between human and animal ears. Fortunately, mammalian ears are strikingly similar in their basic anatomy, even at the cellular level. On the other hand, their sensitivity to sound can vary considerably. Most would contend that the difference in sensitivity is primarily because of differences in the conductive processes that deliver the acoustic energy to the hair cells in the cochlea. For example, the basilar membrane (BM) of the elephant is only a little over twice as long as the parallel structure in the guinea pig, or chinchilla, or cat—animals that weigh only about .03% of the weight of the elephant. A moment's reflection reveals that the structure of the ear, independent of the size of the animal, is primarily a function of the fact that the ear must match the acoustic properties of air if it is to function properly. So ears are similar, in part because they share an affinity for air. But they can differ markedly in how well and in what frequency region they function (e.g., the mating call of the female elephant is a very low frequency signal [which, happily for the elephant, travels far], but it is seldom emitted; so for the male elephant at least, low frequency sensitivity is highly desirable).

In the 1960s—the beginning of our research program—we selected the cat ear as our animal model. It is a reasonable size, the animals were available, and because the cat had long served in the auditory community as an experimental animal, much was already known about it. Other commonly used ears are the guinea pig and the chinchilla, each with its adherents. (In practice, as part of participation in a NATO Research Study Group on Impulse Noise, the French agreed to continue using the guinea pig and the US Army Aeromedical Research Laboratory agreed to continue their use of the chinchilla. There were thus 3 animal models for potential comparisons [NATO 1987].)

Strategic approach – a precis. Given the parallel physiological structures of the human and cat ears, the same electroacoustic model structure would, in principle, work for both. The models for each would, of course, differ in details—different sizes of the elements and so forth—but they would be made up of essentially the same parts arranged in the same way. In order to provide as good a technical and empirical base as possible, we chose to first develop the cat model. Its conductive path could be validated with existing measures and transfer functions. It could also be validated in its ability to predict hazard using noise exposures that actually produced damage—an important test not possible to carry out with human ears.

Once the hazard model was working correctly for the cat ear, the elements in the model could be changed to reflect the structure of the human ear. The conductive path for the human model (AHAAH) could be tested and refined with the available anatomical and transfer functions so that it, too, matched both the magnitude and phase data.

Of course, we could not do the same sort of noise exposures with the human ears; however, we could proceed while making *minimal assumptions* about the correspondence between the cat and human ears. The conductive path for the human model was built on human data. So, from the free field to the stapes, the cat and human models were based on data appropriate to the species. We only needed to assume that the loss processes for the cat and human hair cell were similar. We had reached this point in the mid-1990s, having shared the development of the model(s) and the codes with all interested parties in NATO (Dancer 2003), the US civilian establishment, and the US military (Price and Kalb 1998).

Human noise exposure data. Some noise exposures had been conducted with human Ss and their data (the majority as part of the Albuquerque Studies [Johnson 1998])—both the exposure waveforms and hearing loss measures—were available for analysis. In all, over 70 experimental tests were analyzed (Price 2007). Without further adjustment, the AHAAH model’s predictions (safe vs. hazardous) were correct in over 95% of the instances. Using the same approach, MIL-STD-1474D was correct in 42% of the cases tested (only usable for protected exposures) and A-weighted energy was correct in 25% of the cases. Clearly, the AHAAH model was doing as it should—and doing it far better than the other available methods. Note that the original AHAAH model was *not* adjusted to “fit” the human hearing loss data. Such an adjustment would be a normal part of creating a better model; but so far, there is insufficient evidence that a change would improve the model’s performance. However, in the event that additional data become available that challenge the current version of the model, it should be adjusted to improve its predictive capacity.

4. Basic Modeling Considerations

As we began our modeling, several premises, emerging from basic research on the physiological basis for noise-induced hearing loss, were implicit in our development. Those premises are as follows:

- 1) The external and middle ears were, themselves, relatively immune from damage; however, their acoustic properties shape the energy arriving at the cochlea, the primary site of damage.

- 2) The primary site of the physiological processes responsible for hearing loss is the organ of Corti (OC) within the cochlea (Fig. 2). Even more specifically, it appears that the tip-links connecting the individual “hairs” on the hair cells were likely to be the first elements affected (Fig. 3). BM displacement is the forcing function that drives the OC. Furthermore, the active processes within the cochlea operate at lower SPLs (below 80 dB or so), and the cochlea we were working with at the very high levels was the passive cochlea seen by von Békésy (1960).

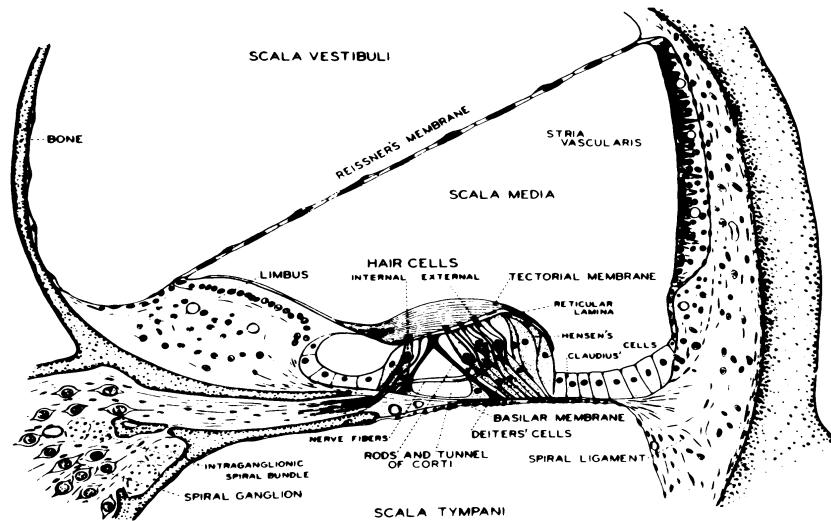


Fig. 2 Cross-sectional view of the cochlea showing the orientation of the BM and the organ of Corti resting on it

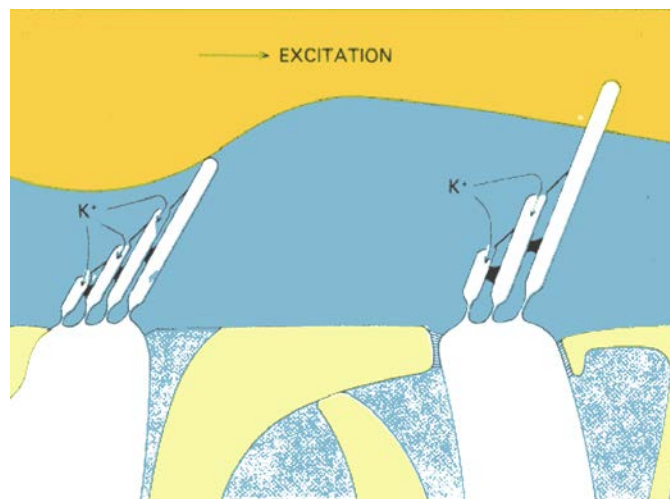


Fig. 3 Diagram showing location of tip links at top of hair cells

- 3) An upward displacement of the BM (on which the OC rests) puts the tip-links in tension (right side of Fig. 3); upward movement is both excitatory

at normal sound levels and is the mode in which tissue tends to fail first (rather than in compression – left side of Fig. 3). The primary loss mechanism is, then, likely to be mechanical stress at the level of the tip-links produced first by upward displacements (related to outward displacement of the eardrum and stapes).

- 4) Finally, the loss processes change character as intensity rises. At lower intensities common to most industrial noises (85–100 dB), they are related to metabolic exhaustion—processes that would recover and could be repeated daily for many years with loss growing slowly over time (Hirsh et al. 1952). Loss and recovery processes at these levels are a logarithmic function of time (Price 1968, 1972; Ward et al. 1959). However, at the very highest intensities, loss processes become essentially mechanical in character. They grow as a *linear* function of time—or number of stress cycles (Price 1968, 1972; Ward 1962)—and recovery is delayed, proceeds slowly (hours to months) (Price 1981), and it likely does *not* go to completion (Hamernik et al. 1988; Luz and Hodge 1971; Price 1983). (As we noted earlier, the intensity realm between the clearly metabolic and the obviously mechanical loss region remains something of a “terra incognita”. The 2 mechanisms must blend in some fashion. At present, we do not know enough to specify any values; but the relationship between the loss and the stimulation is likely to be very complex [Price 1974, 1976].)

Taken together then, the premises suggest that in order to predict changes in hearing from very intense sounds for mammalian ears, we need to focus on predicting mechanical stress at the tip-links of the hair cells from acoustic pressure histories in air.

4.1 Contributions of the Middle Ear

We have noted that the conductive path to the inner ear makes a major contribution to the sound arriving at the cochlea by acting as an acoustic filter. But beyond that, the middle ear introduces a number of critical nonlinearities into the system, considerations that are important in establishing an accurate model of the ear. Specifically, its suspension limits the motion of the stapes (a displacement-related nonlinearity), and the middle ear muscles introduce a time varying nonlinearity that varies with frequency. We will consider spectral tuning, displacement limitation, and middle ear muscle effects in turn.

Spectral tuning. The outer and middle ears act like a bandpass filter, transmitting sound best in the midrange, while cutting off at low frequencies because of stiffness (at about 12 dB/octave), and at high frequencies because of mass (at 18 dB/octave).

These elements are largely responsible for the U-shape of the human audiogram. Alternatively, the relationship between the spectrum of the sound and hazard is complex. Given a rifle impulse and an impulse from a cannon with the same peak pressure (spectral peaks differ by more than 3 octaves), the rifle impulse is much more hazardous, even though measures of energy and duration (used by the traditional hazard assessment procedures) are much greater for the cannon (Price 1983). In essence, the rifle impulse has its energy nearer the midrange where the ear conducts energy well, and the cannon impulse has its energy in the low-frequency region, where the ear conducts energy less well. Accurate representation of the energy actually arriving at the cochlea required that the AHAH model reproduce the conductive path from the free field to the stapes in the time domain (exact patterns of displacement matter). In contrast, the measures of hazard using measures of pressure and duration (MIL-STD-1474D; Smoorenburg 1982; Pfander 1975) take no account of the spectral distribution of energy. The A-weighted energy measure does account for the spectral distribution of energy (where the middle ear is not displacement-limited). Nonetheless, by operating linearly in the frequency domain, at high SPLs the A-weighted energy measure misses critical parts of the ear's response, which, as we have seen, results in inaccurate predictions.

Displacement limiting. Further, basic research indicates that the middle ear becomes a peak-clipper at very high intensities. While it is remarkably linear over a wide dynamic range (up to approximately 130 dBP), there are limits as to how much the middle ear structures can move, a critical issue for hazard assessment (Price 1974). The annular ligament of the stapes, the first element of the middle ear to become nonlinear, limits the stapes displacement to a few tens of microns. In so doing, it produces a strong peak-clipping effect on very intense waveforms. This effect explains why measures not taking specific account of this nonlinearity may correlate with hearing loss at a lower level typical of small arms, yet fail to do so at the higher levels associated with large-caliber weapons. At very high levels, just because the impulse in air becomes more or less energetic by 10 or 20 dB, there is no assurance that the energy in the cochlear input will change by an equal amount. This explains why an L_{AEQ8} of 85 dB will arguably be suitable for rifle exposure, but an L_{AEQ8} of 110 dB will be suitable for large-caliber weapons impulses—a disparity of 25 dB (Murphy et al. 2009; Price 2007). Therefore, in order to reproduce this very important aspect of the ear's physiology, the AHAH model specifically includes a stapes suspension that hardens as a function of displacement.

The level/number trading ratio myth. This same element confounds the existing criteria in that they need to establish a “level/number trading ratio” as part of their formulation. This ratio forms their calculational basis for adjusting for the number of rounds allowable by changing the acceptable peak pressure or vice versa. Given

the reality of the clipping function, it is obvious that there can be no single level/number trading ratio at high levels that is valid (Price 2012). A change in PPL produces different effects on the cochlear input, depending on just how much clipping is occurring (Price 2005) and the level/number trading ratio must change with it.

No other standard includes the refinement of a progressive, amplitude-limiting conductive path. It logically follows that if other standards predict properly for impulses at one level, they must *necessarily* fail at other levels. One might artificially mimic amplitude-limiting by prescribing different criterion levels for different impulses—one level for rifles, another for cannons, and so on. Or, perhaps, some other formulaic trick based on something like A-duration could be devised (such as the one in MIL-STD-1474E). Such procedures are obviously flawed, in that the rules for changing from one level to another are arbitrary. Furthermore, there are impulses encountered in practice, which effectively incorporate elements at more than one level.

In previous years, when it appeared that large-caliber weapons impulses were less hazardous than anticipated, the assumption was made that the hearing protectors worn during the exposures must have worked much better than anyone had previously thought they could (Johnson and Patterson 1993; Smoorenburg 1982). In retrospect, it now seems likely that the stapes displacement nonlinearity was responsible for the smaller-than-anticipated losses seen during those exposures. Under other circumstances it could be disastrous to depend on the apparently “better attenuation” of the HPDs. Clearly, a more sophisticated analytical tool, such as the AHAH model, was needed.

The broader view of “displacement limiting”. The foregoing description of displacement-limiting of the stapes is, at its heart, essentially correct. That being said, however, the displacements of the middle ear at *very* high intensities simply must become very complex and even chaotic. The bones of the middle ear are suspended on ligaments, which, for physiologically reasonable levels, work remarkably well at maintaining their orientation and operating efficiency. But when sound pressures rise above 150 dB or so, it is unlikely that their movements are anywhere near as orderly as at more normal levels (i.e., the stapes can begin to rock about its long axis in the oval window, the incudo-stapedial joint can slide, the ear drum limits displacements, and so forth). Someday it might be possible to describe all this accurately; but for simplicity in modeling, we have allowed the limitation of stapes displacement to stand in for all the “disorderly” processes that occur when the middle ear is overdriven. The essential point is that the energy does not get into the cochlea (where it can do damage to the OC) and it does not establish a “ringing”

in the conductive apparatus. To accomplish this, we also had to include a resistance term (Ramp) in the model that grows in parallel with the stapes nonlinearity.

4.2 Middle Ear Muscle Effects

Lastly, basic research has shown that due primarily to the contraction of the stapedius muscle, the middle ear muscle system produces time-varying attenuation of middle ear displacement capable of reducing energy transmission by 20 or more decibels at low frequencies (below 1000 Hz) and progressively less at higher frequencies. It would be simpler if we did not have to account for these effects; yet they are part of the normal behavior of the mammalian ear and they can and do produce significant attenuations that should be accounted for, especially where very intense stimuli are concerned.

None of the existing criteria, other than AHA AH, make specific allowances for middle ear muscle activity. Industrial noise exposures are largely long exposures to continuous noise, and for an individual ear, a workday's exposure would typically include varying levels and angles of incidence. A detailed accounting of middle ear muscle effects under these conditions would be difficult, especially given the current state of knowledge. However, since we use an A-weighted energy criterion for rating hazard from industrial-level noises (which does not specifically account for the middle ear muscles), an increase in allowable level may have successfully accommodated the general protection they afford.

However, the problem of exposure to weapons noise is dramatically different. An exposure of a few impulses or even a single impulse lasting milliseconds may be sufficiently energetic that it can instantaneously produce serious *permanent* loss. In such cases, the state of the middle ear muscles before and during the exposure is obviously critical, and will have a major effect on the exposure the cochlea receives. The AHA AH model is set up to accommodate an existing contraction at the onset of an impulse or a muscle response that is elicited by the exposure impulse.

Of all the elements in the AHA AH model, the question of its provision for a middle ear muscle contraction has, for obscure reasons, generated the greatest discussion in the technical community. As of this writing, the human middle ear muscle response to gunfire-level stimuli remains essentially undocumented. Recently, Flamme et al. (2015) found that a middle ear muscle response is measurable in 94% of the US population. There are, however, no definitive data regarding whether the middle ear muscles in man are conditioned in people firing weapons (i.e., do the middle ear muscles contract in advance of an impending impulse, if the subject is aware that it is coming and how much protection can be achieved?).

An absence of scientific documentation is not evidence that such a response does not exist. Rather, a few people have been curious about it for many years; but such evidence is not easily or cheaply obtained. Nonetheless, in the creation of the AHAAH model, some position and an appropriate response needed to be taken. If the assumption regarding the protective effect of middle ear muscles is not justified, then the result will be that the model does not fit the hearing loss data. We believe that the preponderance of the evidence is that such a response exists for the human ear. A middle ear muscle response is considered “normal” in the auditory clinic, as it is present in 94% of a normal population (Flamme et al. 2015). Many types of stimuli can elicit a middle ear muscle response—loud sounds, electrical stimulation, puffs of air, stimulation of the face, vocalization, etc.—can all do it. It is not just an auditory reflex, but is part of a set of facial reflexes. So, in the case of intense gunfire, in addition to the acoustic stimulus there are a number of unconditioned stimuli—facial stimuli—that can accompany the sound, each of which could elicit a middle ear muscle response. Unconditioned stimuli abound and the argument *for* the existence of a conditioned middle ear muscle response seemed almost beyond reasonable doubt.

Should an intense stimulus be presented to an ear “unannounced”, there is a latent period in which the nervous system is “discovering” the loud sound and then another interval in which the muscular response occurs (an *elicited* response). The latent period from the arrival of the sound at the cochlea to the onset of muscle potentials can be as short as 9 ms, and the muscle contraction grows at a rate proportional to the intensity of the stimulus (a time constant of 11.7 ms at very high intensities) (Dallos 1964). Typically, their response takes more than 100 ms to fully develop (much longer at the lower intensities used in tests in audiological clinics and most industrial exposure). The usual comment is that the middle ear muscle response is too slow to be protective in the case of something like a weapons impulse. Surely, this is true for a single impulse arriving unexpectedly (gunfire impulses in the free field last only a few milliseconds).

However, there is reason to challenge the simple textbook view. Many impulses (or in practice, even most impulses) are not “unexpected”. The person doing the firing knows he or she is shooting. In the Albuquerque Studies, the experimenters were very careful to include a countdown to the explosion; the second and subsequent impulses in a burst of machinegun fire are predictable, the weapon firer knows the trigger is being pulled, and so on. So the critical question is whether or not the middle ear muscle response in man is conditionable (i.e., can a contraction occur in advance of the stimulus if the owner of the ear “knows” it is coming?) Conditioning *has* been achieved in animal ears and several investigators with a variety of paradigms have demonstrated that the human middle ear is conditionable, as well.

(Brasher et al. 1969; Djupesland 1964, 1965; Yonovitz 1976). Beyond that, the cognitive capacity of the human adds to the probability of a conditionable response. For instance, it has been shown that middle ear muscles contracted as Ss *contemplated* handling a toy that was thought to be noisy (Marshall et al. 1975). The evidence suggests that it is reasonable to expect the middle ear muscles can contract in advance of the auditory stimulus. In fact, it would be difficult to make the argument that we should *not* expect a contraction in advance of the stimulus. Therefore, the model includes the possibility of an anticipatory response, but does not require it.

Additional research on this issue would still be valuable. If the human middle ear muscle response is not conditionable, it would be useful information. If a contraction does occur, it would be good to know how strong it is (the conditioned response might well be weaker than the unconditioned response), how the protective effects might be distributed in the population, how they might be affected by pre-existing losses, and so on. Whatever the findings, the model could accommodate them.

It may not be commonly appreciated, but including the possibility of a middle ear muscle response in the AHAH model is the *conservative* approach to the problem (from the standpoint of protecting the ears of the Soldier). There are 2 ways to think about it. First, by having to choose a calculation where the muscles are precontracted (warned) or not (unwarned), the user of the model can opt for either approach, rather than having to accept a single method of analysis. The unwarned calculation is very conservative.

Second, we note that as the model is presently set up, we assumed that the data from the Albuquerque Studies reflected precontracted muscles. In them there was a clear countdown to the detonation—a stimulus so intense that when an unwarned exposure was tried, the Ss rebelled—they really wanted to brace for the arrival of the impulse (at the highest impulse levels in that test, the Ss referred to the exposure as “a whole body massage”). If we were to make no specific allowance for the muscle contraction, and it *was* occurring, we would have had to account for those data by reducing the sensitivity of the model—making it calculate less displacement within the inner ear and thereby producing a lower rating of hazard. Thus, the readjusted model would allow higher exposures. The problem would then be that the model would underpredict hazard in the case when no middle ear muscle response was present. The non-firer in the presence of a weapon—the unwarned ear—would be at such a disadvantage. In fact, apocryphal stories support this contention: “I was fine until one day a round went off when I wasn’t expecting it; then my ears started to ring and I had trouble hearing anything.” If, on the other hand, the middle ear muscles do not contract in advance of the impulse, then the

model is more sensitive than it has to be—an error of overprotecting the Soldier from hearing loss. The present settings fit the data, while retaining a conservative approach.

Size of the middle ear muscle effect. Given that we were trying to predict hazard for gunfire-level impulses, we sought to represent a median muscle response to a very strong stimulus. In the model the strength of the contraction was represented by a stiffness and a resistance (MemMagK and MemMagR, respectively). The fully developed response is shown in Fig. 4.

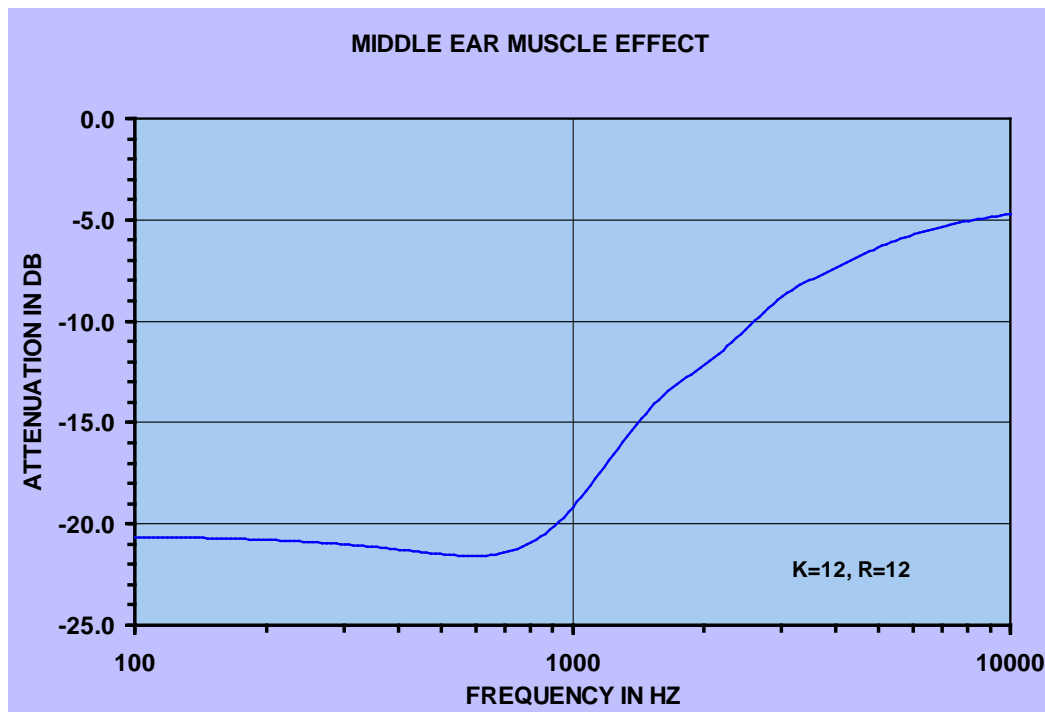


Fig. 4 Attenuation produced by the middle ear muscle contraction in the AHAAH model

The middle ear muscle response. In the AHAAH model, we have left the decision regarding the moment of the onset of the middle ear muscle response up to the user. In essence, the user must decide whether or not the person being exposed is aware that the impulse is coming (i.e., is WARNED) or if this impulse is unexpected (UNWARNED). If it is a WARNED analysis, the model starts the middle ear muscle contraction before the impulse arrives (as the ear would).

If, on the other hand, the impulse is not expected, the model begins its calculation of a changing middle ear muscle stiffness when the impulse triggers the reflex. Establishing that moment requires something of a judgment call. In principle, we seek to set the beginning of strong stimulation that will trigger the reflex. In the case of a simple Friedlander impulse, the leading edge of the impulse is a clear

starting moment. Many times, however, significant stimulation can arrive before the leading edge of a Friedlander wave (and some intense impulses have a different shape). In practice, we argue that a level of 134 dB (100 Pa) is significant stimulation. Thus, the model “expects” the starting point to be 5 ms from the beginning of the wave (i.e., the calculation for the elicited contraction begins at that point). Therefore, the editing programs allow the user to “set start” at a point of their choosing. The model then cuts off the data preceding that point. Then the wave can be stored in that configuration as an “AHA” file.

Additional considerations. As the AHAAH model was first constructed, the idea of including a variable middle ear muscle response was novel and the most practical way of managing it was through the insight of the user. A precontracted response would be appropriate if we were analyzing the ear’s response to a series of impulses close together, such as in a burst of machine gun fire. Also, the model does not specifically include a “relaxation time” for the contraction. The science here is incomplete and so it remains something of a judgment call. This is an area in which additional study would be warranted.

We recognize that there will be a tendency for a user with many impulses to analyze the whole lot through the model and only look at a final result. We are simply not there yet. Each impulse should be examined carefully for artifacts as it is stored for analysis, and the conditions of the exposure evaluated. More work needs to be done before the process can be safely automated.

5. The Model in Quantitative Detail

At the onset of our efforts, the transfer functions from the free field to the stapes were reasonably well known at lower SPLs, giving us the correct expectation that we could accurately reproduce the conductive path to the cochlea for both cat and man, the models with which we were working. Hence, the challenges for a model that worked at high SPLs were, first, to incorporate both the nonlinear elements of the stapes suspension and the middle ear muscle response into the conductive path and, second, to develop an algorithm that reflected the susceptibility of structures within the cochlea.

5.1 The Conductive Path

It remains a surprising thing that the middle ear is linear in its response to amplitudes over an immense range—over a 3,000,000-fold range (130 dB). Nonetheless, gunfire exposures (and variety of bangs and clicks from less bellicose sources) are as much as 1,000 times greater than that. About 40 years ago, Price (1974) calculated that the displacement of the middle ear would be limited by the

annular ligament of the stapes when its displacement reached the 10–20 micron region (at about 130 dB SPL for the lower frequencies). In fact, Guinan and Peake (1967) observed the onset of this peak-limiting behavior in the anesthetized cat ear (see Figs. 6 and 13).

The importance of this peak-clipping element in the conductive chain warrants emphasis. There are 2 major points that should be understood. First, the presence of this critical nonlinearity means that systems for rating hazard that do not account for it will necessarily contain errors—sometimes very large errors. And second, the nonlinearity operates in the time-domain; that is, the peak-clipping occurs at specific instants when the stapes is attempting to move beyond its limits—it is a peak-clipper. It follows that measures that operate in the frequency domain lose the information relating to the timing of events (assuming that just the magnitudes and not phases are accounted for, the typical case). The stapes nonlinearity was modeled as a hardening spring, which ultimately limits stapes displacement.

The middle ear muscle response was modeled as a time-varying stiffening of the stapes suspension produced by the contraction of the stapedius muscle, which mimics the effects as the stapes is pulled sideways in the oval window. The rate of contraction onset as a function of level had been studied by Dallos (1964) and the magnitude by many others; therefore, we were able to incorporate a time constant and magnitude of response typical of a normal ear.

5.2 Cochlear Susceptibility

The question of how to evaluate intracochlear factors was problematic. In principle, one could begin with the anatomic details of the OC, which is a complex mechanical structure, with elements that range from stiff to gelatinous to liquid. One might try to make estimates of the multiple unknowns, their physical properties, their interactions, susceptibility to fatigue, etc., and build a damage model from the bottom up. However, because the living OC is inaccessible, its structure is both delicate and mechanically complex, and critical data on its properties were essentially unknown, the risks of making estimates on all these parameters were huge. Some other approach was needed.

We, therefore, adopted an alternate approach to characterizing loss mechanisms within the cochlea. Our approach was empirical. Auditory theory had progressed to the place that BM displacements could be calculated, given a waveform at the stapes. Therefore, we decided to allow data from controlled exposures to describe the relationship between mechanical displacement and threshold shift.

For the calculation of BM displacement, we modified a fast method developed by Zweig et al. (1976). The cochlea is modeled as a 1-dimensional fluid-filled transmission line with exponentially tapered cross-sectional area and BM width. In the modeling coefficients section of this report (the MAN.COE file), it is referred to as a “Type 2 model (WKB taper)”. The original Zweig et al. version was a constant-Q model (unlike the real cochlea); therefore, we adjusted it to be a constant-loss model (like the real cochlea, with Q growing from apex to base).

In normal ears operating at lower SPLs, positive feedback effects from the outer-hair cells give rise to cochlear amplification; but at high levels—above 80 dB or so—the cochlea is again linear but is much less sharply tuned. Therefore, because we were concerned with predicting the effects of very intense sounds, we used a linear WKB solution for the complex displacement transfer function as a function of driving frequency. This calculation transfers frequency components of the stapes displacement with amplitude and phases given by a Fourier transform analysis of the stapes displacement history into magnitude and phases of components at 23 equally spaced locations on the BM (between .425 cm and 3.175 cm from the basal end [dimensions for the human cochlea]). The resulting BM displacement histories are obtained by an inverse Fourier transform of these frequency components at each location.

Calculating the active cochlea. As an aside, we note that the decision to model the cochlea without active processes was based on the reality of the ear’s response to very high levels of stimulation. The AHAH model incorporates a term (Ca for “cochlear amplifier”) that makes the model useful at other intensities, as well, should any researcher want to use it for other purposes at lower levels. If Ca is set to 0.5, the waveforms match those of the cochlea without the active processes that exist at lower levels. (If it is set nearer to 10, the waveforms have a much higher “Q” and “ring” like the BM does at lower levels where the active processes have their effects.)

The damage calculation. At high SPLs (well above 115 dB), hazard within the cochlea can be thought of as analogous to mechanical fatigue. Indeed, at very high levels, it is generally agreed that the ear appears to be “torn up” rather than “tired out”. In the literature on mechanical fatigue of materials, failure is predicted by keeping track of the number of flexes and their amplitudes—raised to some power, typically 2 or higher (Broch 1979) (Bcoef in the MAN.coe file). Therefore, we calculate hazard at each of the 23 locations for which a displacement history was just determined by establishing the maximum upward BM displacement between successive zero-crossings (peak of a flex cycle), squaring the value (in microns) (Bcoef = 2), and summing it for the location (upward displacements put the tip links in tension—see Fig 3). The resulting value has been named “auditory risk units”

(ARUs), which we set out to relate to temporary and permanent hearing loss in the cat ear (Price 2003).

By focusing on BM displacement, this rationale deliberately sidesteps the specific question(s) related to the detailed damage processes within the OC. On the other hand, BM displacement is the forcing function that is causing the stresses with the OC and as such should be causally relatable to hazard to hearing.

Empirical tests of the cochlea's response. Given the common structure of mammalian cochleas and the considerable knowledge that had been developed with respect to the cat ear in particular, we exposed anesthetized cats to a variety of intense impulses. Anesthetization had the critical effect of eliminating both movement of the ear during an exposure (which would change the transfer function) and inactivating the middle ear muscle reflex, which had been shown to have a major effect when the cat was unanesthetized (Price 1991).

In testing the hearing of the cat, we used electrophysiological measures of sensitivity—the nerve response measured from scalp electrodes on anesthetized animals. This response is similar to an auditory threshold in an awake, behaving animal, and is much more easily measured.

A technical aside. For more than 50 years the auditory world has accepted pure tone thresholds to be the gold standard of auditory system function. If, following an exposure, there was no change in the pure tone threshold, the ear had not been permanently affected. There had also long been concern that this presumption was problematic. There was no incontrovertible proof that pure tone thresholds were all that one needed to measure; but the argument did have face validity, there was no other alternative, and research needed to go on. Kujawa and Liberman (2009) have demonstrated that following a 2-h, 100-dB, exposure to an 8–16-kHz octave band of noise, the mouse ear shows threshold shifts that recover; yet at the same time, it demonstrates physiological damage at the level of the hair cell—neural junction and neural degeneration. Thus, we can no longer blithely assert that no change in pure tone threshold is proof of an intact, unaffected system.

At the same time, those studying noise effects have not been entirely insensitive to the possibility that recovered thresholds might nonetheless be hiding some trauma. In fact, Pfander (1975) viewed a delayed recovery of threshold as indicating trauma and others have agreed. In that regard, we note that the changes observed in the Kujawa and Liberman work showed “recovery” taking a couple of weeks. Thus, a delayed recovery seems likely to be a sign of some permanent change in the auditory system.

That being said, there is still a question as to what the correspondence is between the mechanisms of loss observed by Kujawa and Liberman (2009) in response to an intense band of noise operating for 2 h and the processes associated with *much* more intense impulses delivering the same or greater energy in 10 or 20 ms (weapons impulses). In the case of the band of noise, the loss mechanisms would be likely to be associated with metabolic issues, and in the case of the more intense weapons impulses, the changes would be a function of mechanical stress. In both cases, it is likely that recovery would take place over several weeks. The conservative approach would argue that the prolonged recovery could be related to the possibility of permanent changes, even if the recovery were to pre-exposure levels. It would be scientifically interesting for someone to conduct a parallel study to Kujawa and Liberman's, with exposure to high-level impulses.

While it is interesting to note the work of Kujawa and Liberman, which cautions us that noise exposures can have subtle, deleterious effects, it is interesting to note that Hamernik et al. (2003) have, for example, demonstrated that noise exposures of about the same severity as those of Kujawa and Liberman, have a protective, toughening effect on chinchilla ears. Clearly there are complex, interesting processes going on here and much more work needs to be done.

In all, 12 different impulse exposures were employed in validating the cat ear model (Pierson et al. 1995; Price and Kalb 1999; Price et al. 1995; Price and Wansack 1989; Price 2003). The specific impulses used in the exposures were selected to challenge the ear with very different types of stimulation that would provide critical tests for model development. In order to promote at least face validity and avoid the problem of justifying simulations of stimulating events, all were produced by explosive sources found in military settings. In order for exposure data to be most useful, they need to produce some loss at their lowest levels and not produce total destruction in all the ears at their highest levels. In the case of intense impulse exposures, this window is relatively narrow because once an exposure reaches a level that begins to produce loss in a given ear, a relatively small increase in intensity can result in total destruction of the cells in the ear. All our exposures achieved this goal.

The test exposures. The exposures were chosen to test the effect(s) of specific conditions; therefore, we'll briefly discuss each of the exposure types and the theoretical challenges each provided.

It seemed reasonable to suppose that the ear would be most susceptible to impulses that put their energy where the ear was tuned best—the 4.0-kHz region. We tested this possibility by exposing ears to 50 impulses produced by the primer in a rifle round. Its A-duration is very short, about 80 μ s, and as a result its spectral peak was

at 4.0 kHz. Groups of ears were exposed to 50 impulses at 135, 140, and 145 dBP (Price and Wansack 1989).

There were 2 tests of an exposure to a single round from the AR-15 rifle at the firer's ear position. In one case the weapon was standard, and in the other the muzzle device (flash-hider) had been replaced with an experimental muzzle brake. The 2 impulses had the same spectral distribution of energy; but because the muzzle brake reflected gasses backward, it produced 13-dB higher peak pressures and a 10 dB increase in energy. These impulses provided a critical test of the effect of the stapes nonlinearity (as predicted, the hazard was equal for the 2 conditions in spite of the difference in peak pressures and energies).

In order to include exposures to larger numbers of rifle impulses, we used 4 different conditions: 50 impulses at 140 and 145 dBP at 90° to the angle of fire (most of the energy in the initial peak) and 2 exposures (6 and 12 impulses) at 4 m and 200° to the angle of fire (144 dBP). Moving to the rear produced an exposure in which most of the energy was in the latter part of the impulse rather than the peak. These exposures checked for impulse complexity and increased numbers of rounds.

Finally, we used 3 different single exposures to airbag noise—a complex impulse of a type that, while interesting in their own right, might also be produced by a round penetrating a crew compartment (Price and Kalb 1999). In those exposures, the peak pressures ranged from 167–173 dB, but the shape of the impulse was not like gunfire. The hissy filling of the airbag took place in the cab of a pickup truck under 3 different conditions: 1) the windows were open, 2) the windows were closed, or 3) the windows were up and the compartment was sealed with tape. The differences in the venting of the compartment varied the low-frequency component(s) in the waveform. The inflator noise took about 80 ms and its pressure history interacted with the condition of the passenger compartment. Thus, the compartment had little effect when the windows were open, and when the compartment was sealed there was a large low-frequency component present as the airbag inflated in the unvented space. The closed compartment was an intermediate condition. These exposures tested very intense stimulation and particularly challenged the part of the model that dealt with amplitude limitation of the stapes displacement.

All these exposures were run and the immediate (half-hour-plus) and permanent losses established. The immediate losses are referred to as compound threshold shifts (CTS) because they contained both temporary and permanent components. In response to lower levels of stimulation, the immediate recovery processes are sizable and complex, hence the exact time of measurement of a TTS is critical. On

the other hand, the ear's response to these very intense stimuli tends to be relatively stable for a matter of hours (Hamernik et al. 1988). This meant that the exact time of measurement was not critical.

5.3 Opportunities to Adjust the Model

The place/frequency map. It has long been known that the cochlea performs a frequency analysis of its inputs, with the low frequencies having a maximum response at the apical end of the BM and the high frequencies at the basal end. Fortunately for the modeler, Greenwood (1990) has reviewed the frequency-position data for several species, among them the cat and man. It seems that cochleas behave in essentially the same way across the frequency range to which they are sensitive. This meant that the cochlear model's frequency/place map simply needed to correspond to the research on frequency location within the particular cochlea. That being said, there is an inherent uncertainty with respect to the "correct" location of effects. We now know that under normal circumstances the active processes in the outer hair cells effectively "stiffen" the responsive cells, tuning them to a higher frequency. For example, cells that in the absence of active processes would resonate to 1000 Hz, would, as a result of the active processes, resonate best to a higher frequency—in the vicinity of 1500 to 2000 Hz. This is the explanation for the "half-octave shift" upwards in the frequency of maximum threshold shift when the ear is exposed to fatiguing stimuli. Internal features of the AHAH model allow it to reproduce both the active cochlea and the cochlea without active processes (and anything in between). As it happens, the frequency/place maps come from research in which the active processes are present and the frequency/place provisions of the model could be adjusted to match the data.

This inherent uncertainty with respect to the exact location of the action of particular frequencies should cause no real problem in assessing hazard. Typically, research is done with threshold testing at octave frequencies and, thus, threshold shift measures are not highly focused on exact frequency locations. Nor need they be—the energy distribution in intense stimuli is relatively broadband (as are the losses). In fact, because the head and middle ear effectively create a bandpass filter, experiments show that small arms, rockets, and cannon impulses, while having their spectral peaks in different frequency regions, all produce losses in the ear's midrange. The ear is more sharply "tuned" than the spectra of the impulses. So the area in which the ear is tuned best receives the greatest stimulation. Thus, in general, there is no compelling theoretic reason to agonize over predicting the loss at a specific frequency. Then, too, there are the practical considerations associated with testing at more frequencies. The additional tests required for a finer analysis

take more time and long sessions of threshold-tracking do not necessarily produce better data. So all things being considered, an octave-band analysis of effects is reasonable and it does result in tests at roughly equally spaced intervals along the BM. Note that AHAH's analysis is at roughly one-third octave intervals.

There is the associated question of the frequency content of the signal at the level of the cochlea. The middle ear is remarkably linear; but at about 130 dB at the lower frequencies, we have seen that it stops being a linear conductor (see Price 1974). And at even higher pressures, such as those in impulses from firearms, the stapes can peak-limit inputs or the middle ear can vibrate in modes that do not transmit energy to the cochlea. So even if the transfer functions from the free-field to the tympanic membrane are valid—air, itself, becomes nonlinear at high pressures, and knowing the frequency content of the energy arriving at the cochlea is problematic.

Issues associated with the nonlinear stapes. Given that the frequency/place map was reasonable, we then had the opportunity to adjust the model's other parameters to arrive at the best description of the data. As mentioned earlier, the conductive path from the free field to the stapes displacement (at normal sound levels) had been adjusted to produce transfer functions that fit the measured performance of the cat ear. On the other hand, the model included certain variables that could only be estimated. For instance, the model included a term ("Ramp" for Resistance amplification) that was intended to represent properties of the ossicular chain when it was driven into nonlinearity at SPLs over 130–140 dB (Price 1974). The energy arriving at the stapes needed to be accounted for, as it had to go somewhere. It seemed reasonable to propose that there are processes that act to dissipate energy through motions not along the normal conductive path (the resistance). The middle ear is suspended on ligaments that simply must allow the middle ear to move in nontraditional ways at very high SPLs, such as the side-to-side rocking movement of the human stapes observed by von Békésy (1936). Actually, in the case of the human ear, the annular ligament is not uniformly wide (the anterior ligament is wider than the posterior ligament [Bolz and Lim 1972])—which, under normal circumstances, would argue for a slight rocking motion about that axis). While it is certain that such dissipative movements exist for the stapes (Gyo et al. 1987; Hato et al. 2003; Heiland et al. 1999; and Lauxmann et al. 2014), it is highly unlikely, even today, that they could be modeled for all the ossicles in sufficient detail to be useful in the present circumstances. Our resolution to this problem was to propose a dissipative nonlinearity that would begin to act for large stapes displacements and be proportional to the amplitude of the displacement. That being said, the value of "Ramp" simply had to be estimated and adjusted to fit the hearing loss data.

We also used another approximation in calculating the stapes response. The measured area of the stapes footplate is 3.2 mm²; however, the value we actually

used in AHAAH was 2.1 mm^2 , a deliberate choice to reflect what we believe is the *effective area* for a human stapes operating at very high amplitudes. The rocking motion is likely to produce a radiation pattern that approaches that of a dipole, which is less effective than a simple piston. Therefore, in the interest of simplicity, sometimes held to be a scientific virtue, we opted to use a smaller area for the stapes' footplate for calculations at these very high levels.

5.4 Stapes to BM Transfer Functions

In the end, the basic modeling question is what the transfer of displacement from the stapes to the BM looks like. The transfer functions for pure tones of different frequencies from the stapes to locations on the BM are presented in Fig. 5.

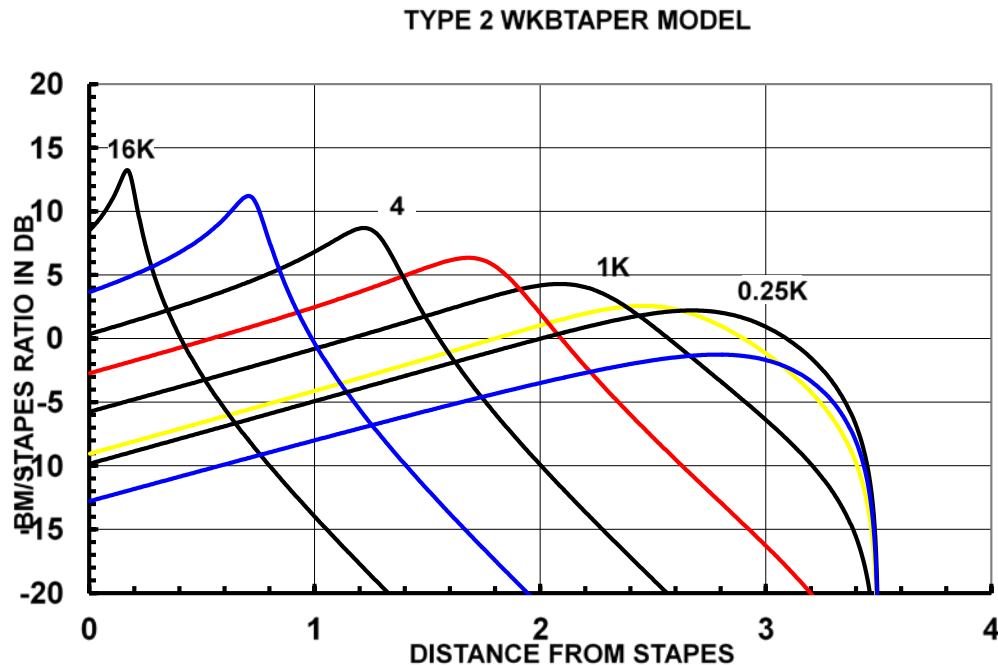


Fig. 5 Transfer functions in the AHAAH model for stapes displacements to basilar membrane displacements for pure tone stimuli

Hazard on the BM. In similar fashion, we also had to create a model of hazard at the level of the OC. We believed that the problem could be usefully characterized as a “fatigue of materials” process. If so, we needed to keep track of the number of flexural cycles and their amplitude. Therefore, at each of 23 evenly spaced locations along the BM (roughly one-third octave intervals), the model seeks the peak of an upward displacement (in order to establish a peak, the waveform must rise to a high level, then decline to the rest position). The peak displacement (in microns) is then raised to some power (the B-coefficient) and the result stored as the “dose” at that

location. As a reading of the fatigue of materials literature and the argument by Broch (1979) indicated, the likely value of the B-coefficient should be near 2.0 or a little higher.

5.5 Confronting the Model with Data and Adjusting It

In the scientific method, the modeler is entitled to his or her premises; but in the end, the theory is tested by its ability to predict the relevant data. Our baseline data were the hearing loss data from the 12 different exposures, and the modeling challenge was to find the combination of model elements that produced the greatest order in the threshold shift data (while maintaining the fits to the transfer-function data already described). The mean loss for each group was taken as representative of the group's loss (this was reasonable given that the mean and median losses were similar). So the challenge was to adjust the remaining variables—Bcoef, damage threshold, memMagK, MemMagR, cochlear gain factor—so that we achieved the most reasonable fit to the threshold shift data. Then the question was whether or not the model's calculated risk in ARUs matched the loss data and did so better than other methods of assessing hazard.

In fact, we were able to achieve a remarkably good correspondence between the group mean CTSs and the model's predictions in ARUs. The fit can be seen in Fig. 6. The correlation of $R = 0.94$ implies that 89% of the variance is accounted for, an excellent fit to the data. Additionally, the formula for the least-squares fit allows one to predict the CTS for any number of ARUs:

$$\text{CTS} = 26.6 \times (\text{LN}(\text{ARU})) - 140.1$$

Note that the ARU calculation is done for all 23 cochlear locations, but the output of the model, when in use as a standard, gives only one number—the highest ARU value (as noted earlier, in all cases so far seen, in the midrange of frequencies). Health hazard assessment is focused on preventing *all* PTS, hence we report the highest risk. (In fact, for the sufficiently curious, the software will write all 23 values as a table if the user changes the appropriate toggle in the MAN.coe file).

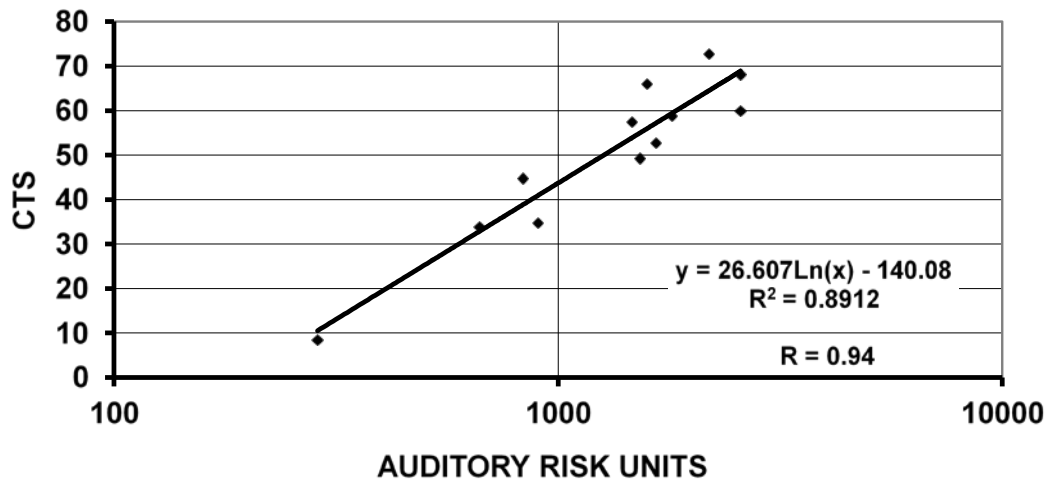


Fig. 6 CTS for 12 experiments with the cat ear (see text) exposed to impulsive sounds as a function of the auditory risk units (ARUs) calculated with the AHAAH model of the cat ear. Each data point represents the mean loss at the frequency showing greatest loss for both ears of 10 cats. The trend line represents the least squares fit to all the data.

There is also a reasonably well-established relationship between CTS from these intense stimuli (the result of underlying mechanical damage), and PTS and hair cell loss (Price 2006b). Data from the cat indicate that for stimuli at these levels, about 0.6 to 0.8 of the CTS will become PTS (full recovery taking a month or 2).

The relationship expressed by this empirically established formula can be thought of as characteristic of mammalian cochleas. We believe that this clear result was in part a function of the fact that the conductive path of the cat was well known and the middle ear muscle system was *not* active. In essence, under these conditions, we were observing essentially pure cochlear phenomena.

The data in this figure are key in understanding the prediction of loss with the AHAAH model. They are taken as the generic response of hair cells—human or cat—to intense stimulation. They were gathered without middle ear muscle involvement and no allowance for individual differences in susceptibility. The good fit between the predictions and the losses suggested that we had the basis to create a human model—AHAAH.

5.6 Accounting for Individual Differences in Susceptibility

In virtually any experiment in which more than one S is tested, we observe differences in the dependent measures. In the discussion thus far we have been calculating the “typical”—mean or average—response of the ear as being representative of the processes we are interested in. Yet, we have long known that if a population of ears were exposed at a level that would affect the average ear in

a moderate way, we will measure a range of losses, with some ears showing much larger losses, while others may show little effect. For both practical and theoretical reasons, there has been an interest in quantifying the susceptibility of the ear to hearing loss (e.g., Henderson 2006; Henderson et al. 1993; Kujawa and Liberman 2006; Marshall et al. 2006; Price 1998, 2010; Summerfield et al. 1958; Tempel et al. 2006; Ward 1967). Of particular interest in the present context is the common observation that the variability is especially high in the case of impulse noise (Henderson and Hamernik 1986).

Considerable effort has been expended since the 1960s in looking for some measure of intrinsic susceptibility. It would be a boon to hearing conservation if such a factor or factors could be identified. Initially, various tests of threshold shift were sought that could predict susceptibility for exposure to industrial noises (see reviews by Kryter 1970 and Ward 1967), efforts that proved largely unsuccessful. In the intervening years and with new technologies available, the search for sources and indices of susceptibility has continued (see for example Henderson 2006; Henderson et al. 1993; Marshall et al. 2006), with the result that a great many factors can be conceived of as possibly being associated with susceptibility—middle ear muscle responsiveness, sex, chemical exposure, prior exposure to noise, eye color, inner ear protective responses, genetic factors, oto-acoustic emissions and so on.

With respect to exposure to very intense sounds, such as gunfire, very much less work has been done, in part because it is such a difficult area in which to work. Underlying the difficulty is the fact that at very high levels the loss mechanisms become fundamentally mechanical in nature. Hence, losses can be immediate and recovery prolonged and uncertain. Nonetheless, our need to understand these issues is acute. Over 40 years ago, Hodge and his coworkers (Hodge et al. 1965; Hodge and McCommons 1966) ran a number of studies using repeated (up to 10 repetitions) exposures to 7.62-mm rifle fire (25 or 50 rounds at 155 dBP or 158 dBP) (12–29 Ss). They concluded that while the group TTSs and standard deviations (SDs) were repeatable, individual TTSs were not consistent enough to permit generalizations. More recently, an analysis of the Albuquerque data set indicated that susceptibility is not a constant within an ear (Price 2010b), a finding that is consistent with the work of Hodge and his colleagues. Ward (1962), likewise, found that the variability of his Ss response to intense impulses (produced by a speaker [peaks above 155 dB]) was so great that no meaningful conclusion could be drawn with respect to susceptibility.

Part of the reason for the failure to establish a relationship has surely been a lack of theoretical grasp of the processes that contribute to susceptibility. A few moments' reflection reveals that these processes, broadly conceived, can include not only the

many factors previously mentioned but psychological dimensions, as well (e.g., willingness to wear hearing protection, being alert to incipient impulse exposures and so on). In the case of impulses from explosive sources, even an element of bad luck in being near a hot spot in the explosive cloud or at an unfortunate distance from a reflective surface that would promote a larger TS in an individual ear, as would a momentary break in the seal of an HPD. Surely it is important to understand these elements if we are to deal with them quantitatively in arriving at a DRC for very intense sounds.

For hazard assessment associated with intense impulses, these differences in response to exposure are critical. For exposure to typical industrial noises (85–100 dBA), hearing loss grows slowly over a number of years and monitoring tests can detect a progressive change in threshold. With intense impulses, however, the effects can be rather like falling off a cliff—an exposure to one impulse can produce large permanent losses. Vause and LaRue (2001) documented an unfortunate case in which a Soldier in training fired one round from a rocket launcher while not wearing his hearing protection and suffered a large PTS that ended his budding military career.

As a matter of convention, in establishing noise standards, we currently try to protect the 95th-percentile ear. It would be nice to protect *all* ears, but 95% is accepted as the highest protection that is practical. The formula for hazard relating AHUs to CTS was developed empirically and is a prediction for the 50th-percentile ear. In order to be able to predict for the 95th-percentile (most susceptible) ear, we adopted the following rationale. As our earlier discussion has argued, many things—currently unspecified—could affect the susceptibility of a particular ear. We, therefore, decided to model the following principle: a susceptible ear, for whatever reason, is like an average ear being driven harder. In addition, we made the assumption that susceptibility, like so many elements in life, is normally distributed. The problem was to relate the percentile of susceptibility to the concept of being driven harder. That was a question that could be related to the data we had.

Being “driven harder” is like being exposed to an impulse at a higher SPL. Therefore, in the model, we could artificially alter the SPL of the impulse and recalculate the hazard. From a modeling standpoint, the question was how much change in pressure was needed to replicate the response of the 95th-percentile ear. We therefore assumed a variety of SDs—4, 6, 8, 10 dB—calculated the hazard and compared the resulting predictions to the actual data. If the number was too small, then the model predicted lower losses than the data showed or vice versa; too large a number and the model predicted losses when the data showed none. The result of this exercise in examining the data was that a SD of 6 dB seemed to match the data best. And it is also true that many things in the auditory world—thresholds, for

example—have about a 6-dB SD, so this value had the virtue of being reasonable, as well. Given that a 95th-percentile ear is, by definition, 1.64 SDs from the mean, AHAH was set to predict the 95th-percentile ear by first raising the SPL 10 dB and then doing the hazard calculation. (In operation of the AHAH model, this manipulation is, of course, transparent to the user.) An advantage of this approach is that the same logic could be used to predict the hazard from any other percentile of the population desired.

5.7 Creation of the Human Model

The conductive path. The first order of business in creating a model for the human ear was to adapt the values in the conductive path of the basic model (Fig. 1) from those appropriate to the cat ear to those that fit the human ear. The fits for both magnitude and phase were quite good for the path from the free field to the cochlear input (Figs. 7 and 8).

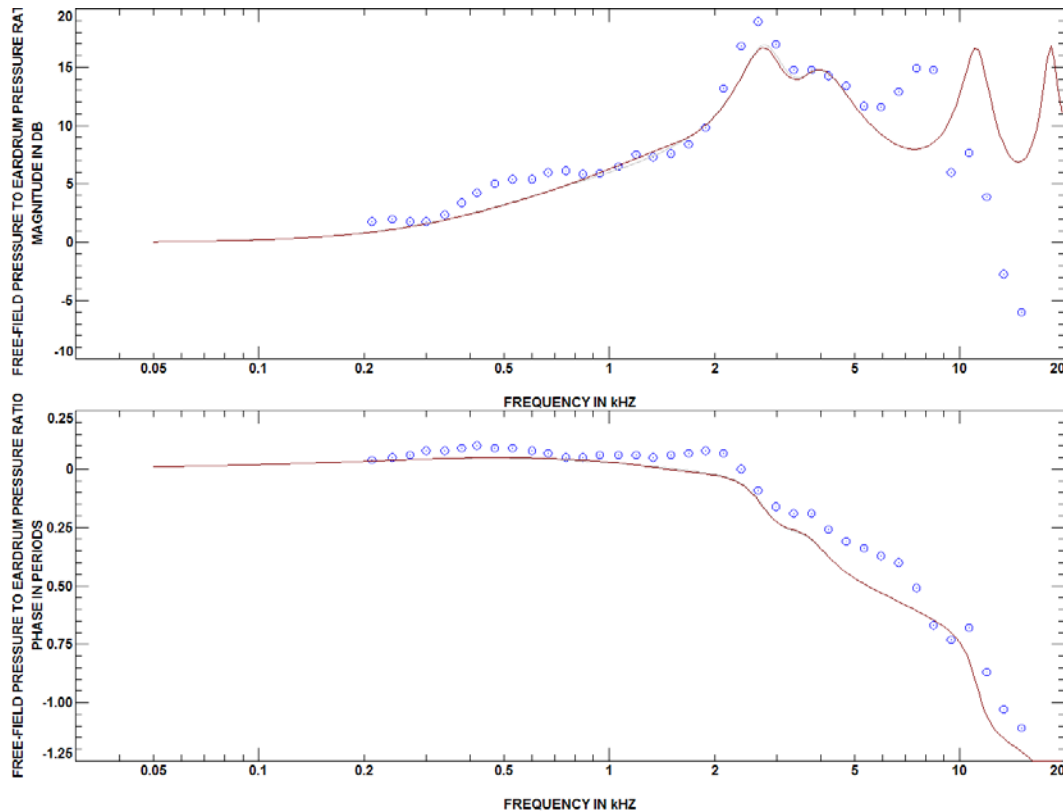


Fig. 7 Transfer function for free-field pressure to pressure at eardrum. Magnitude appears in the upper panel and phase in the lower panel. The dots are data (Mehrgardt and Mellert 1977) and the lines are the calculation by the model.

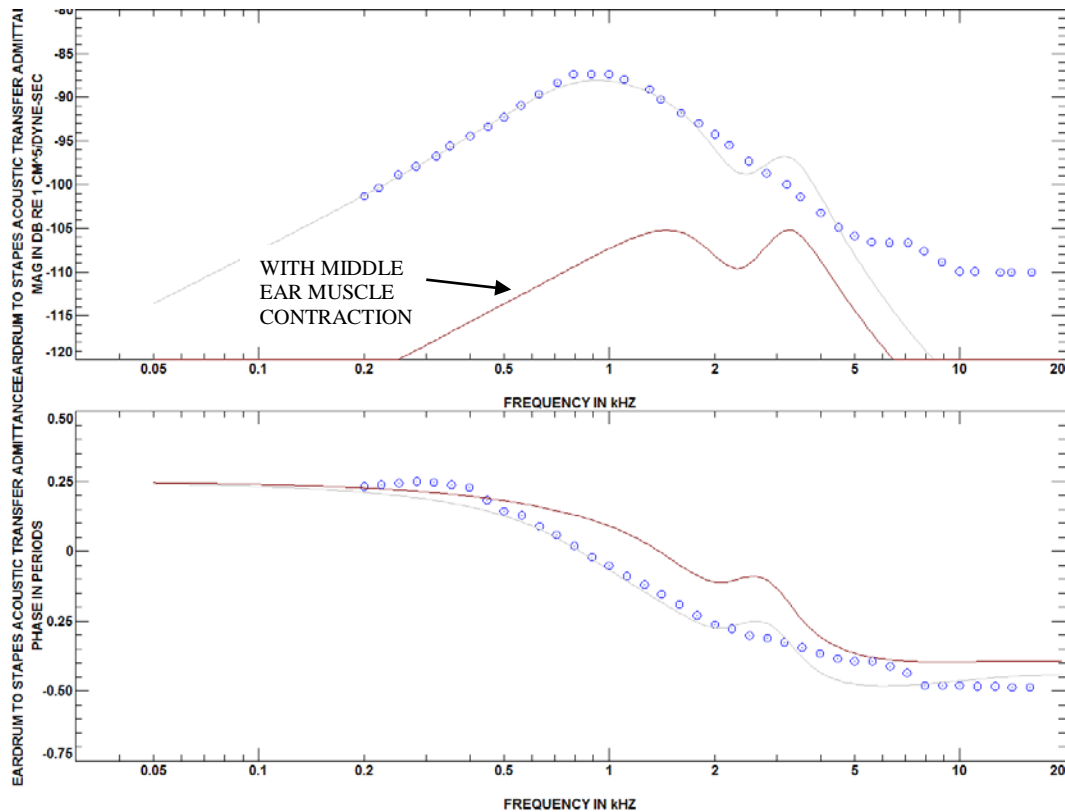


Fig. 8 Transfer function for eardrum pressure to stapes volume velocity. Magnitude appears in the upper panel and phase in the lower panel. The dots are data and the lines are the calculation by the model. Transfer function data from Kringlebotn and Gunderson (1985).

Middle ear muscle effects. In developing the model for the cat, the anesthetized preparations assured that no middle ear muscle activity occurred. Thus, we had a relatively pure test of the conductive path and intracochlear factors. In applying the model to real situations, however, we need to properly account for middle ear muscle activity. We can allow the middle ear muscles to contract in advance of the arrival of the impulse (a warned exposure) or we can allow the impulse to “elicit” a contraction (an unwarned exposure). Given the very intense exposures for which we are rating the hazard, the model was set to provide a short latency (Mem delay = 9 ms and a rapid growth in contraction strength, MemTimeConstant = 11.7 ms, consistent with the work of Dallos [1964]).

Size of the middle ear muscle effect. Because we were trying to predict hazard for impulses with peak pressures well over 140 dB, we sought to represent a median muscle response to such strong stimuli. In the model, the strength of the contraction was represented by a stiffness and a resistance (MemMagK and MemMagR were each set to 12). The attenuation produced by the fully developed response has been shown earlier in Fig. 4.

The Cochlear Gain Factor. For obvious reasons, there are no data for the normal human ear relating BM displacements to stapes displacements. And because there are constraints on human use in experiments, it is unlikely that such data will ever be available. In any event, the AHAH model includes a link—the CochlearGainFactor in the MAN.coe file—that allows one to adjust the relationship between stapes displacements and the BM displacements that the model calculates (see Fig. 6). With no clear guidance, we again followed a logical path to an approach. If we assume that hair cells function similarly in both the cat and man, then it would seem to follow that the same stimulating conditions ought to exist at threshold in the region of best sensitivity—the 4 kHz region—for both ears. Therefore, the CochlearGainFactor was set so that, given a particular stapes displacement, the AHAH model produces the same displacements in the midrange of the cochlea as does the parallel model for the cat ear.

5.8 Additional Features of the Model

Inclusion of HPDs. The theoretically based approach adopted made it possible to provide a variety of useful features not currently found in DRCs. For instance, the model allows its calculations to start at 3 locations: the free field, at the ear canal entrance, or at the eardrum location. Waveforms can be recorded at any of these locations and the model can begin its calculation with the appropriate algorithms. This property allows several useful features to be realized. For example, a recording made at the ear canal entrance allows the hazard calculation to account for issues associated with specific angle(s) of incidence (perhaps uniquely the same for a firer whose eye is at the sight, but variable for others in a firing team), or it allows an analysis of the complexities of a reverberant environment. In addition, it might allow calculation of the most favorable angle of incidence (e.g., a crewman might be told to face in a particular direction or assume a particular posture that reduces the hazard). Or in field deployments, the user might want to avoid (or seek) reflective or absorbent surfaces. Further, the choice of inputs beginning at the ear canal entrance or the eardrum means that HPDs can be integrated into the hazard calculation. Of course, measurement at the eardrum position presumes the use of an acoustic manikin, which brings with it a host of other technical concerns; but it does provide a waveform. As of this writing, there are serious reservations concerning the validity of waveforms measured with manikins. We do not have data that would allow a definitive comment at this point. However, our suspicions are that isolation of the measurement microphone from “the back path” (paths bypassing the path through the hearing protector) may be a serious issue. Alternatively, it is possible to calculate the effect of an HPD on the input waveform (Fedele and Kalb 2015; Kalb 2010). There are in fact, many sources of variance

associated with HPD use—poor fit being a prime example. But whatever choice is made with respect to how HPDs should be included, the AHAAH model is capable of incorporating a wide range of approaches.

An A-weighted energy criterion is also capable of using measurements made on an acoustic manikin and processing the measured waveform. There is potentially a large error inherent in such a use, however. The shape of the A-weighting filter assumes free-field stimulation of the human ear. Thus, it includes all the acoustic effects from the free field to the eardrum (about 18–20 dB in the midrange). If pressures are measured at the eardrum position in a manikin, then, in effect, the amplification produced by the barrier effect of the head, the pinna effects and the ear canal resonance, are essentially being counted twice.

The other criteria use single-number adjustments to account for HPD effect, an approach that simply ignores the large and what we now know are the increasingly complex effects of HPDs. Nonlinear HPDs, such as the combat arms earplug, are increasingly being used by troops because they provide both protection and allow for situational awareness. Obviously, single-number adjustments for HPDs do not effectively represent these devices. And if the pressure is high enough, even normally linear devices can become nonlinear. Fortunately, the AHAAH model simply needs a waveform to do its calculation; therefore, recordings acquired on an acoustic manikin or calculations done with a mathematical model of the protector could provide such a waveform.

Analysis of the growth of hazard. A second type of novel feature included with the AHAAH model is a movie that shows the calculated action of the waveform within the cochlea. For low-level exposures to continuous sounds, such a display is not particularly useful. During a long exposure at lower levels, such as one that may occur in the workplace, many things vary—middle ear muscle state, angles of incidence, HPD fit and so forth—and the growth of risk is relatively slow. But in the case of very intense impulses, where the exposure to damaging energy may occur in milliseconds, the details of the action can be critical. By stepping through the waveform and the hazard calculation in parallel, the movie can show exactly what part of the waveform had the greatest influence on hazard and what did not matter. Such information can provide engineering insight into ameliorating or eliminating the hazard. For example, as mentioned earlier, in the case of airbag noise exposure in a closed passenger compartment, the movie revealed that the high peak pressures were not transmitted to the cochlea because of the peak-clipping effect of the stapes. In another case, the movie showed that the physical “bounce” of the airbag away from the Ss face—by bringing the pressure down to normal atmospheric levels where the ear could conduct normally for a few milliseconds—was material in increasing the exposure by about 75% and creating a dangerous

exposure. Conversely, restraining the bounce would reduce the hazard to safe levels (Price 2006). In the same vein we see that for an exposure to a cannon-like impulse at a relatively low level—where the middle ear is essentially linear—hazard, like the energy, is primarily in the initial impulse and the latter part of the impulse contributes little to the hazard. At high levels, on the other hand—where the middle ear is decidedly nonlinear—little of the hazard comes from the initial part of the waveform, even though most of the energy in air is there. But most of the hazard now comes from the last part of the waveform—still at a high level and where the middle ear is operating in a nearly linear fashion. Successfully combating hazard with some ameliorative scheme depends on understanding these relationships.

It is ironic that for 50 years, hazard evaluation schemes focused on only the energy near the peak pressure and ignored the tail-end of the impulse, and we now discover that what really matters may be the very part we have been ignoring. Perhaps we have been saved by the tendency for large peaks to have large tails, as well—so “more” is generally worse; it is not likely, however, to result in insightful engineering fixes to the problem.

5.9 “Hidden Features”

In the ancient and respected traditions of DNA codes and evolution, the software of the AHAAH model includes vestiges of its developmental past. The evidence of these codes resides most visibly in the MAN.coe file. Some of these subroutines are presently unused or their functions are fixed. However, in the future there might come an occasion when certain exposure conditions might arise such that their specific features might offer “survival value” and they could be implemented. We will consider 3 of these.

Stress weight base/Stress weight apex. One of these features is the SweightBase /SweightApex values (Stress-weight at the base of the cochlea and Stress-weight at the apex of the cochlea). Because the BM changes width systematically along its length, it seemed reasonable to suppose that a given peak displacement (what the model calculates) in a narrow membrane region might be more stressful than the same displacement in a region where the BM is wide. These values are multipliers (1 means no effect and the ratio of the values for the base, and apex implies a progressive emphasis from one end to the other). While the basic idea behind the concept still seems reasonable, we have left both the values at 1. We did this first for simplicity and second because any choice of values would have been essentially a guess that we had no real way to test. The problem was that our data set used for establishing the relationship between ARUs and CTSs did not really test such a provision. The reason is that the tuning of the conductive path to the cochlea is

relatively sharp compared to the spectra of the noises to which we exposed the ear (or is normally exposed to in a wide range of instances). As a result, the largest losses—both CTSs and PTSs—are seen in the midrange (where the ear is tuned best) and under those conditions, the stress-weighting scheme would have little effect. In addition, in the one case for which we have data with a relatively narrow spectral peak (spark-gap discharges), the AHAAH model's prediction of lessening hazard as the spectral peaks moved to higher and higher frequencies (above 3.0 kHz and up to 16 kHz) agreed with the data from the human exposures (Loeb and Fletcher 1968).

Damage Threshold. A second feature that is present but unused is the “DamageThreshold.” In essence, it seems reasonable to assume that there must be some minimum displacement of the BM that is too small to represent a serious mechanical stress, or alternatively, so small that the metabolic mechanisms within the inner ear can keep up with the demands present and do not add to the hazard. It, too, seems like a reasonable idea; but in the interests of simplicity (and because it had no apparent effect on our data) we have left it set to 0 (all peaks are included in the analysis). This could conceivably get to be an important issue if AHAAH is used to evaluate the hazard from much lower intensity sounds.

Angle of incidence correction. For an impulse recorded in the free field, hazard assessment protocols require that the angle of incidence with respect to the ear is presumed to be the worst-case angle (coming from the frontal quadrant). Therefore, the AHAAH model includes a subroutine that calculates the waveform arriving at the ear canal entrance given a free-field impulse at the microphone location. This subroutine is adapted from the work of Bauer (1967) and has 4 variables—the real and imaginary parts of the induction sound field and the real and imaginary parts of the radiation sound field—that can reproduce the head-related effects (in the horizontal plane) that are present in coming from the free field to the ear canal entrance.

These routines would be very useful should we be concerned about other angles of incidence. For example, good hearing conservation practice would recommend that members of a firing crew might wish to face in the least hazardous direction (probably looking away from the impulse source). Such effects can be relatively large and are not likely to be operationally prohibitive. As the model is presently configured, this feature is not available; but the code is in the software.

The belt and suspenders approach. We again note in passing that calculating the hazard for the 95th-percentile ear *and* assuming the worst-case angle of incidence is likely to produce a value that is somewhat on the high side. Thus, we have chosen to err in the direction of overprotecting Soldier's hearing.

And does it work for the human ear? Once the model had been adjusted to produce a good fit to the transfer function data available for the conductive path and adjusted to fit the “mammalian cochlea” for its response to intense stimulation, it needed to be tested against all the available data on hazard for exposures of the human ear. The expectation was that this comparison would show that the model did not fit certain exposure conditions and would need to be readjusted to produce a better prediction. The positive outcome was that this comparison of the model’s output with the hearing loss data showed that the model was predicting very accurately (Price 2007). The somewhat more than 70 cases examined were from many years of tests in different labs. Not surprisingly, the tests were not run in parallel fashion, so a rigid statistical analysis was not possible. Nonetheless, the same type of analysis was used to test predictions using MIL-STD-1474D, an A-weighted energy measure, and AHAH to identify both safe and hazardous exposures. Whatever the weakness of the statistical procedure, it was the same for all the methods tested. The AHAH model predicted correctly in over 95% of the cases, the MIL-STD-1474D was correct in 42% of the cases (protected hearing only), and A-weighted energy was correct in 25% of the cases. Errors for all methods tended to be in the direction of overprediction of hazard. Clearly, the AHAH model is getting the right answer far better than other methods.

Given the high accuracy of the model, as of this writing, no changes have been made to the original human version. That being said, a number of different “versions” of the program have been used; in each case, however, they were developed to do some useful thing, like processing a number of impulses in a “batch”. The essential algorithms still do the same thing and report the same result.

An additional point to note – a need for “dither”. Full disclosure of changes in the program requires that a caveat should be noted. In order for some of the mathematical processes to work properly, the data being analyzed must include at least *some* variability. For example, if in storing or editing a file, a string of zeros was added to bring a data file up to a particular size, the zeros represented a challenge to the mathematical algorithms that require at least some variability to process. We have, therefore, included an algorithm that provides a very low level numeric “dither” to the data (at least 96 dB below the peak level). This represents an insignificant change to the data, but it does mean that outputs of 2 runs of the same impulse might differ in the last decimal place.

5.10 Dealing with Protected Hearing

It seems likely that most noise exposures will occur to ears that are wearing some hearing protection (at least that is the official desire of the hearing conservation

community and, interestingly enough, of the combat arms community as well). That being said, for many applications there is interest in hazard to the unprotected ear (e.g., virtually all noise exposures to the noise of airbag deployment will occur to unprotected ears). The AHAH model, as we have discussed it, has shown its capacity to predict threshold shifts for ears that were unprotected and also to predict for those ears that were wearing protection (Price 2007). This was possible because the data we had from the Albuquerque studies included waveforms recorded at the ear canal entrance, under the muff used in the study.

The version of AHAH approved for use with MIL-STD-1474E provides for the effects of hearing protection in 2 ways: 1) Measurement of the protected waveform or 2) Calculation of the protected waveform.

Measurement of the protected waveform – a further look. The AHAH model can also handle the hazard to protected ears through the use of an acoustic manikin that would allow input waveforms to be measured. For a variety of reasons, an acoustic manikin would be an invaluable tool. As noted earlier, it would allow the evaluation of complex noise fields where there may be specific angles of incidence that characterize the exposure (e.g., crewmen might be facing away from the muzzle of the weapon). Also, rounds are seldom fired in a free field. Troops try not to expose themselves to enemy observation or fire and as a result, they fire from defiladed positions. In those cases, the reflected waveforms could represent a major part of the exposure and the angles of incidence matter. The acoustic manikin would allow such effects to be evaluated.

Still, however, an acoustic manikin introduces uncertainties of its own. Does it match the properties (impedance, temperature) of human skin properly, are its physical dimensions proper, does it get the bone-conduction path correctly (Berger and Kieper 1967), is the microphone robust enough, is it isolated sufficiently, do the impedance-matching elements of the middle ear respond appropriately at high levels, etc.? These are real problems. A recent paper by Zagadou et al. (2016) failed to address serious errors associated with the use of a manikin (Price and Kalb 2016). Unfortunately, at the moment there is no agreed-upon standard manikin for use at high intensities; but a manikin could provide realistic waveforms.

Calculation of the protected waveform. In the event that the waveform cannot be measured at the ear canal entrance or at the ear drum location, another alternative remains. MIL-STD-1474E provides the capacity to calculate the waveform under typical hearing protective devices, given a free-field pressure. AHAH's calculation of HPD effects on the free-field waveform requires yet another model. We address this procedure next.

5.11 HPD Performance Measures

Direct physical measures. A little familiarization with the applicable technical jargon can help to clarify this discussion. HPD performance can be characterized through a variety of measures, some of which are purely physical and others that include the use of human Ss. The apparently straightforward physical measures include the use of an acoustic test fixture (ATF) (which may be a manikin) on which the test HPD is placed, or a microphone positioned under a protector worn by a human being (a microphone-in-real-ear [MIRE] measurement). However, there are serious questions as to how well ATFs simulate the real interactions between a human being and a protector. Alternatively, the MIRE method does require that a small microphone be fitted under the protector and it follows that a wire must exit through or beneath the seal of the test protector, a procedure that includes the possibility of a leak pathway or the conduction of sound from outside the HPD to the area under the HPD. Simple physical measures are really not so simple.

Measures using human Ss. An alternate method requires the active participation of human Ss to arrive at an attenuation value. In essence, Ss are immersed in a sound field and their thresholds are determined for one-third octave bands of noise for at least the center frequencies of 125, 250, 500, 1000, 2000, 4000, and 8000 Hz (ANSI S.12.42 2010). Then the test HPD is fitted and the thresholds are redetermined, hence the “real ear attenuation at threshold” (REAT) test. The difference between the 2 measures is taken as the attenuation of the HPD (Berger 2005).

The REAT measurement provides what is referred to as the “insertion loss” (IL) for the protector. In passing, note that as the name indicates, the measure is made at the hearing threshold of human Ss. If the HPD is linear in its response, then the attenuation values remain the same as the level of the sound field rises. Fortunately, most protectors are linear over quite a wide range of intensities—up to gunfire levels (155 dB or so). Above that level most plugs stay linear and muffs, with their large volumes, may become nonlinear (Buck 2009).

Two alternate nonlinear possibilities can exist. First, if the pressure is high enough—especially for a muff-type protector—the protector might become nonlinear (not attenuate as well as before). In extreme circumstances, muff-type protectors may physically move on the head or even be sprung away from the ear in response to the low-frequency negative pressures in the impulse. Second, some protectors are deliberately designed to be nonlinear in their response. That is, they attenuate little at lower intensities (where the wearer might want to maintain “situational awareness”). Then at higher intensities, the attenuation can be made to increase, where the wearer needs protection from very intense impulses. This type

of nonlinearity can be the result of acoustic elements designed to limit transmission at high intensities, or alternatively, the protector may contain electronic circuits that conduct at low levels (or even amplify it) and limit transmission at high levels. In either case, the REAT values are obviously limited to applications at levels where the protector's response is linear.

The nonlinear protector has grown in favor within the combat arms community because it promotes situational awareness—needed for survival in combat—and at the same time, it protects the ear from hearing loss when intense sounds are experienced; this, in turn, acts to maintain sensitive hearing for situational awareness. As we will see later, these protectors provide a special challenge when we try to incorporate them into a hearing hazard analysis using AHAH.

First, consider the analysis of the effects of linear protectors. REAT data are available for many HPDs and represent something of a “gold standard” for attenuation assessment. However, knowing the REAT values does not tell you what the *waveform* actually looks like for any given impulse. The waveform is what the ear actually experiences (given that it operates in the time domain), hence that is what AHAH needs in order to perform its analysis. The challenge for the analysis of hazard with AHAH is as follows: knowing the REAT values for a protector, being able to predict the waveform under the protector for any incident impulse. Some method of calculating the input waveform from the free-field pressure would be useful as a “front-end” for the AHAH analysis.

5.12 The Hearing Protection Module (HPM)

Enter yet another model. Our HPM is also an electroacoustic model, but this time reproducing the behavior of earmuffs and earplugs (Fedele and Kalb 2015; Kalb 2013). Electroacoustic models have long been used for hearing protectors (see for example Schröter 1983; Schröter and Pössl 1986; Shaw and Thiessen 1958, 1962; Zwislocki 1957).

Modeling the conductive paths. Arguably, there are 3 important energy-flow paths associated with a protector which determine its attenuation properties: 1) air-leak paths at the contact points with the skin, 2) the protector moving as a rigid piston supported by its contact with the skin, and 3) transmission through the protector material, itself. In the HPM, each energy flow path is modeled as an independent piston working into the occluded volume (OV) behind the protector. For each piston there is 1) an associated resonant frequency, 2) a “quality factor” (Q) that characterizes the sharpness of the resonance, and 3) a low-frequency limiting effect below the resonance and 4) a high-frequency cutoff of 18 dB/oct above it. The 3 paths are presented in a circuit diagram in Fig. 9.

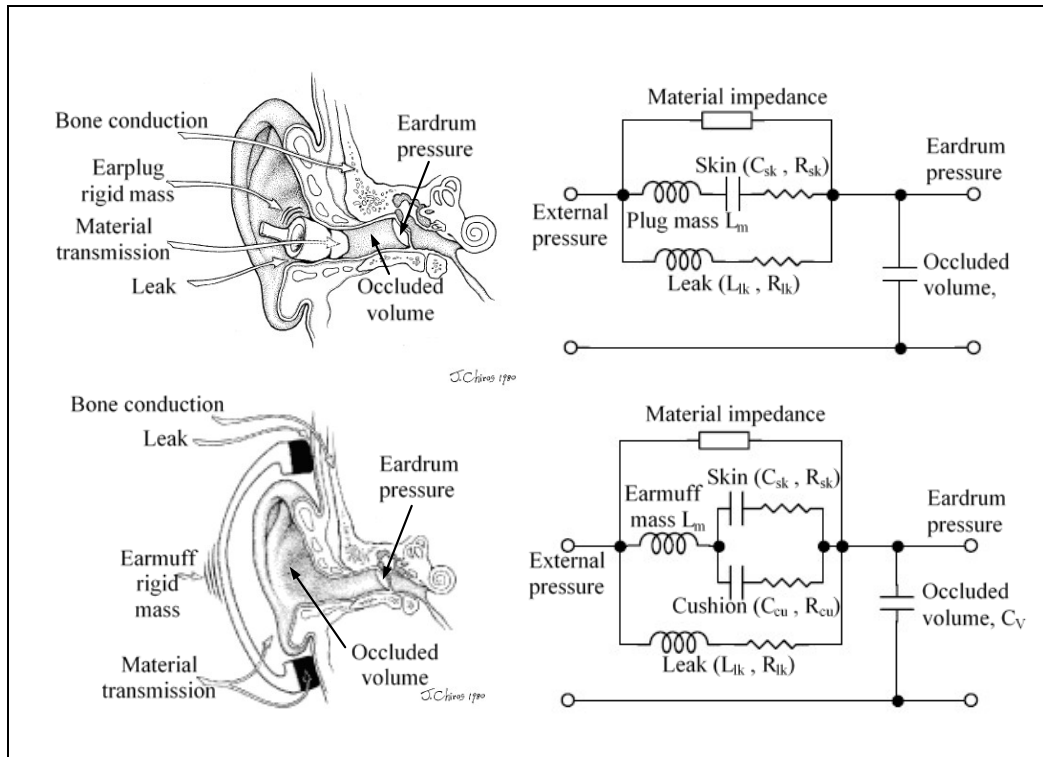


Fig. 9 Circuit diagram of the 3-piston model of a hearing protective device

Physical locations and qualities of the paths. Interestingly—and fortunately for our purposes—each path dominates in a separate frequency region. The air-leak piston is largely a very low-frequency feature having its important effects typically between 0 and 63 Hz; though, for a large leak the resonant frequency might be as high as 1 to 2 kHz. For this piston, the attenuation at 0 Hz must of course be 0 dB (ultimately atmospheric pressure changes will get into the occluded volume (OV), for even a small leak). The mass of this piston is that of the plug of air particles moving in phase. The resistance is due to the viscosity of air moving past the surfaces surrounding the leak path and because the damping is typically high, it follows that the Q-factor is low, typically around 0.5 (if, per chance, the mass and resistance form a Helmholtz resonator in conjunction with the OV compliance, the Q-factor might be as high as 3).

The second piston, formed by the mass of the leak-free protector moving as a rigid piston supported by its contact with the skin, moves under pressure from the external sound to compress the OV behind the piston, producing sound pressure at the eardrum. Its resonant frequency is typically in the midrange of frequencies, 1–2 kHz, and its low frequency attenuation is in the 20–30 dB region, depending on the stiffness of the skin cushion support and the acoustic compliance of the OV.

The Q factor for this piston can vary from 0.5, for a highly damped piston, to 2.5 for a lightly damped piston. At higher frequencies, the 18 dB/oct cutoff applies.

The third piston accounts for the transmission through the material of the HPD, itself. The resonant frequency for this piston is between 4 and 8 kHz. The material damping can vary over a wide range, giving a Q between 0.2 and 10. The “support” of this piston can be very stiff (depending on the compliance and resistance within the protector material), hence the low frequency loss can range between 20 and 40 dB. Again, the high-frequency loss follows the 18 dB/oct curve.

In passing, we note that we ignore the bone-conduction path, as well as the path through the seal of the protector. We believe that their effects are negligible compared to the transmission along the other paths.

Kalb (2013) has demonstrated that this model can fit virtually all the individual REAT values that were produced in the round-robin standardization study by Royster et al. (1996). These data included self-fits by 384 inexperienced Ss, which produced a very wide range of REAT values.

For analysis using AHAH, a set of values can be found for the protector under evaluation. That being done, it is possible to process any waveform with the HPM and calculate the pressure history that would exist under the protector having those particular REAT values. Thus, we have a method for providing a waveform under a protector for AHAH to analyze.

In passing, we note that nonlinear HPD responses can also be modeled. If data indicate that protectors become nonlinear at high intensities, then nonlinear elements are incorporated in the model (Fedele and Kalb 2015). For example, earmuff cushion stiffness increasing with compression could be described by a cubic displacement term added to the linear displacement term in the rigid piston path. Or if the flow resistance increases with increases in the volume velocity, then a cubic flow velocity term is added to the linear velocity term in the leakage path.

As of this writing, MIL-STD-1474E includes 11 different hearing protection options, namely those held to be typical by the health hazard assessors (combat arms plug, linear; combat arms plug, nonlinear; COMTAC III muff; etc.) (note that 2 of the 11 are duplicates, but used under different operational conditions).

As an acknowledgement to the practical hearing conservation world, the REAT values used in the calculations with the HPM in MIL-STD-1474E have been de-rated by 1 SD as a “conservative” assessment of the protectors’ attenuation. This has been and continues to be the practice on health hazard assessment within the US Army.

6. The Problem of Which Standard to Apply for Protected Ears

The AHAAH model is designed to deal with the risk of hearing loss due to high level exposures—exposures at levels for which the primary loss mechanism is essentially mechanical stress at the level of the hair cell. Unprotected exposures to most firearms fall in this category. Once the peak levels fall below 140 dB or so, however, it is less certain that AHAAH fits. MIL-STD-1474E addresses impulsive noise only at levels greater than 140 dB.

As the level falls, as previously noted, the damage mechanism within the ear changes and recovery processes begin to operate (not specifically accounted for by A-weighted energy). We have entered the “terra incognita” of the hearing loss phenomena. Research needs to be directed here. That said, in the zone where the stapes is essentially linear, for pink noise, AHAAH and A-weighted energy are very close in their rating of hazard for free field exposures. In the absence of the nonlinear stapes, AHAAH is essentially an energy model (at the level of the hair cell).

6.1 Mathematical Aspects of the AHAAH Model

The AHAAH model was developed as an electroacoustic analog of the ear, designed to predict hazard from intense sounds. In it, the physiological and acoustic elements of the ear have been translated into their electric analogs. This relationship is diagrammed in Fig. 10. Regions of the ear moving in phase, such as the bones of the middle ear, are approximated by a lumped-parameter circuit element. More complex or extended objects, such as the ear drum, the ear canal, or the cochlea, have been subdivided into sections that are small compared to the highest frequency of interest (hence, move in phase), or else they have been modeled as transmission lines. For example, the eardrum is divided into a nonconductive part and a conductive part connected to the ossicles.

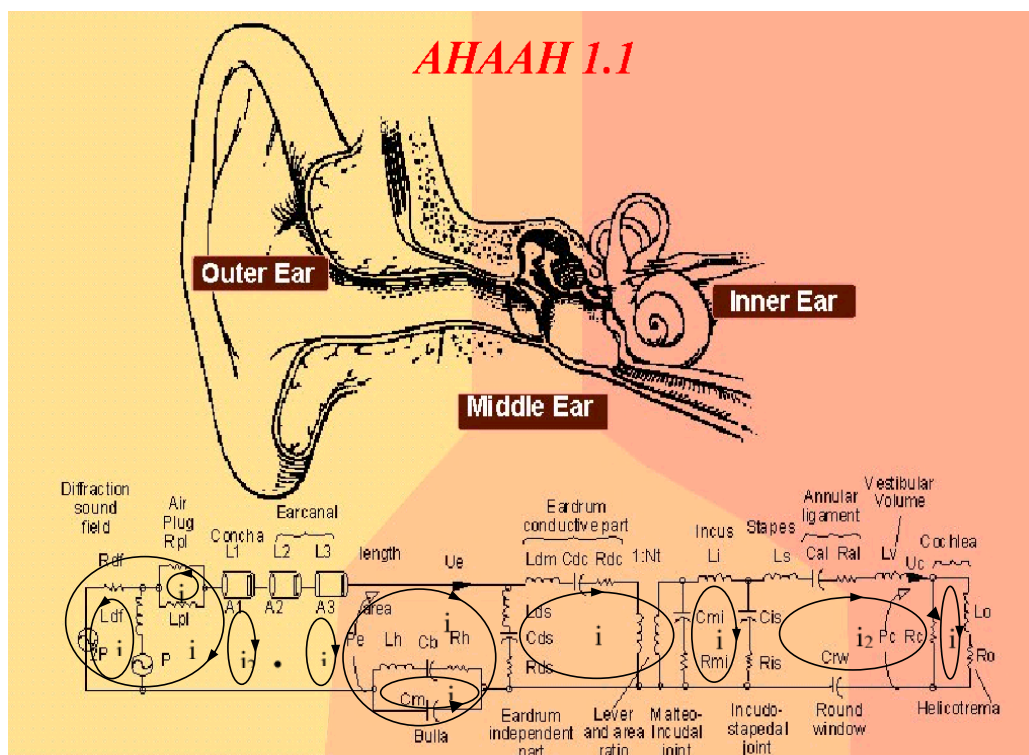


Fig. 10 Diagram of AHAH, an electroacoustic analog of the ear

Setting the values for the variables in the model. For almost all physiologically normal levels the middle ear is essentially linear; therefore, in developing the model we calculated the input impedance and transfer functions of the model ear, and compared them with transfer functions measured for the human ear. The values of the model's components were adjusted so that they were reasonably close to average physiological values, and at the same time maximized the goodness of fit to the magnitude and phase data in transfer functions measured for the human ear by other investigators.

In using such an adjustment procedure, the specific values chosen might deviate somewhat from rigidly defined anatomical values. By analogy, a condenser microphone might have a physical diameter of a half-inch; but because its diaphragm is constrained at the rim, it is most compliant at its center and its effective diameter might be somewhat less than the half-inch nominal dimension. In choosing the specific values for the model's variables, we emphasized maximizing the goodness of the fit between the model's analysis and the measured transfer functions. In the end, we wanted to predict the energy actually entering the cochlea, and that seemed like the best approach. At the same time, we recognize that, given the large number of anatomical variables in the model, many alternate sets of values could be developed. In the end, however, the question needs to be,

first, whether or not the fit to the transfer functions is improved and, second, whether the modification provides an improved fit to the data on hearing loss.

Adjusting the model. In the process of creating and adjusting a model, one makes one's best estimates and then tests the resulting model against some appropriate, empirically derived data set. At that point it is possible to see how well the model has predicted the data. Typically, there are some areas needing adjustment, the model is altered and retested. Such was our expectation. As 2016, we have seen nothing that suggests that such adjustment is necessary.

This state of affairs is possibly due to 2 different circumstances. First, the precursor model for the cat ear was tested on a wide range of impulses deliberately chosen to test the model's provisions—temporary-to-permanent losses were produced in biological ears. The high correlation between the model's predictions and the measured hearing losses ($r = 0.94$) suggests that the basic model was well formulated. Secondly, in the case of the human model, there is a relative paucity of hearing loss data to analyze. No one sets out to produce PTS in humans. Furthermore, there is very little TTS data even from major efforts, such as the Albuquerque Studies. In all the ABQ testing (2000+ exposures), fewer than 30 threshold shifts in the 15–25 dB region were produced (Price 2010b). Those studies told us that much of the stimulation was safe; but we have little threshold shift data demonstrating what represents a hazard. And even in this case, the AHAAH model predicted hazard correctly in about 95% of the cases (Price 2007)—far better than the other standards that have been evaluated. It seems likely that the model could be improved; but at the moment, we have no data that would suggest the changes that are needed.

The results of these calculations appear in Figs. 11 and 12.

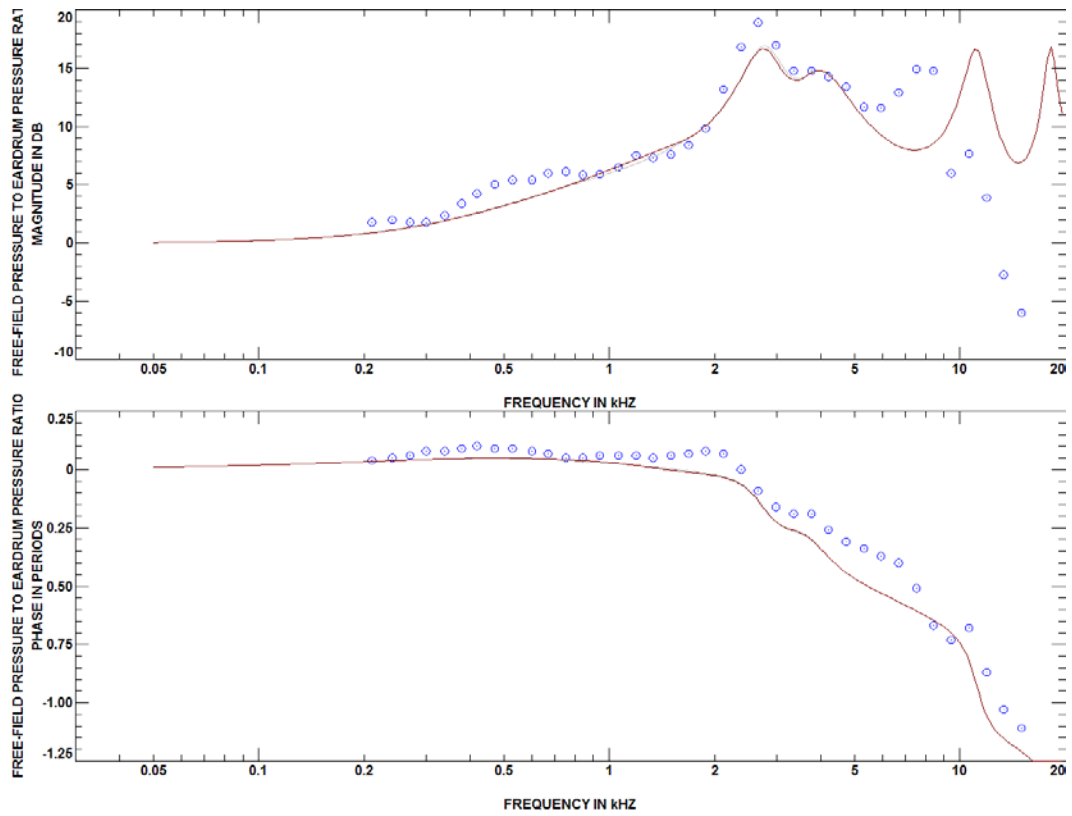


Fig. 11 Transfer function for free-field pressure to pressure at eardrum. Magnitude appears in the upper panel and phase in the lower panel. The dots are data (Mehrgardt and Mellert 1977) and the lines are the calculation by the model.

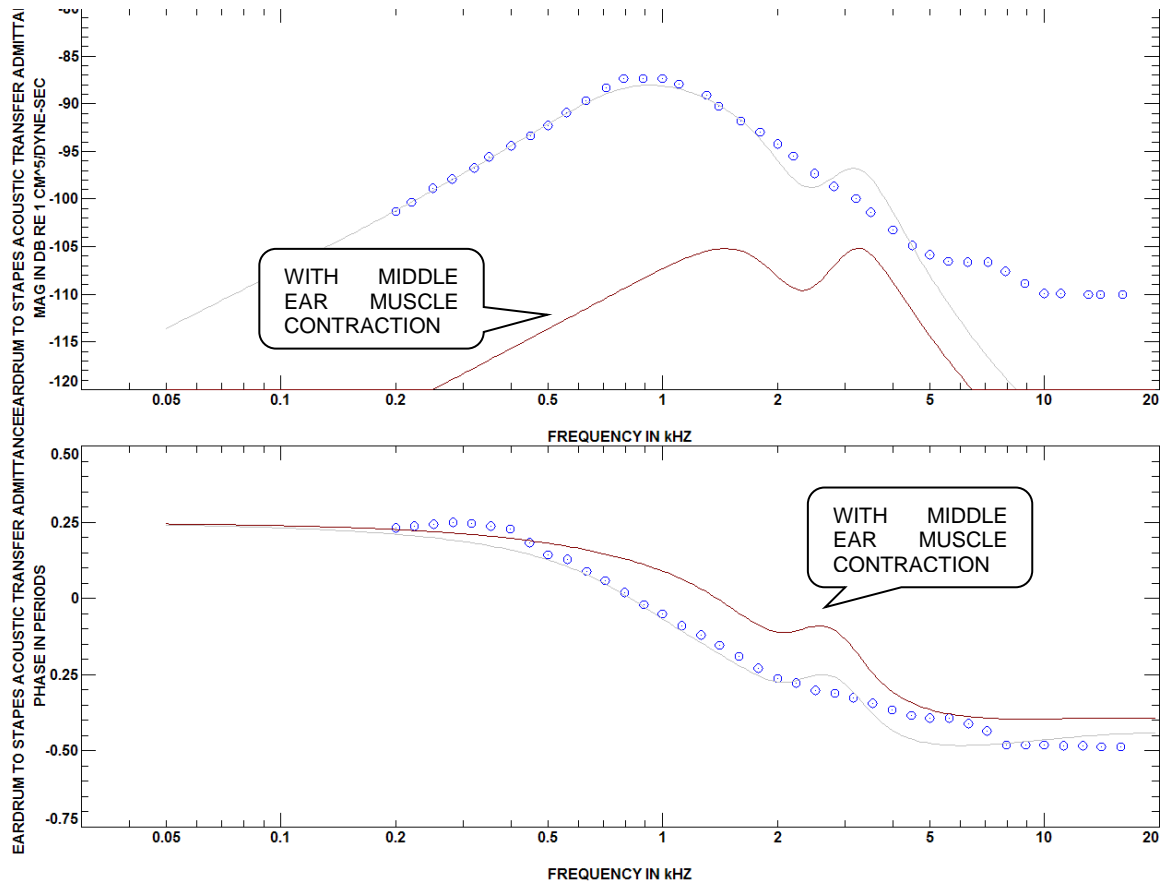


Fig. 12 Transfer function for eardrum pressure to stapes volume velocity. Magnitude appears in the upper panel and phase in the lower panel. The dots are data and the lines are the calculation by the model. Transfer function data from Kringlebotn and Gunderson (1985).

The nonlinear middle ear. At very high stimulus levels, some of the elements depart from their linear values. In addition, in order to reproduce the effects of the middle ear muscles, some elements are required to vary with time as well. The critical elements in this regard are the stapes and its suspension in its annular ligament (Guinan and Peake 1967; Price 1974). Nonlinear behavior of the annular ligament has also been observed by Zhang and Gan (2014). Of all the parts of the middle ear, this element reaches its limit of physical displacement earliest. At the same time, the ligament is structurally rugged enough to stop stapes displacement. Thus, it sits as a peak-clipping controller and gatekeeper of input to the cochlea. The primary damage processes are located within the cochlea.

To calculate the effect of this peak-clipping nonlinearity, we break the problem into 2 separable pieces—one nonlinear part before the stapes and a linear cochlear section after the stapes. For a given pressure waveform, we numerically integrate the set of coupled nonlinear differential equations to get a solution for the stapes displacement. To maintain accuracy and prevent numerical overload, we have used

a fourth order Runge-Kutta method with an adaptive step-size control. To check accuracy, the method doubles the number of steps, repeats the integration, and compares the results. If the error is too large, the step size is halved, and the calculation and comparison are performed again. This stepping algorithm monitors the velocity of elements in the vicinity of nonlinear components and adjusts the step size to maintain the worst-case percentage change in velocity below the acceptable limit. We further stabilize the solution by allowing viscosity to proportionately follow the stiffness in the annular ligament. This has the effect of dissipating energy that would otherwise result in “ringing” of the system and physically reflects the fact that the middle ear, at very high levels, can vibrate in modes that are not part of the normal conductive path, dissipating energy.

The annular ligament is modeled as radial springs displaced tangentially to their axis, much as they would be on a trampoline. A tangent function describes their “constitutive relation” for the Young’s modulus.

The action of middle ear muscles is superimposed on the foregoing calculation. The stapedius muscle is responsible for most of the effects on the conductive path; therefore, its action is modeled. When it contracts, it pulls the neck of the stapes sideways and causes the annular ligament to stiffen. This results in a relatively large attenuation (20 dB) of frequencies below the middle ear’s resonance (about 1 kHz) and less attenuation at high frequencies (tapering to 5 dB). The reflex is taken to have a latency of 9 ms and a time constant of 11.7 ms. For the “unwarned” calculation, the reflex calculation is started 5 ms into the pressure history, and for the “warned” condition, the calculation assumes that it is at full strength at the beginning of the pressure history.

We note that the area of the stapes footplate used in the AHAH model is somewhat smaller than the actual dimensions of the footplate. This choice was something of a modeling compromise, based on observations of the particular patterns of motion observed in human ears. The human annular ligament is unlike the cat annular ligament in that it is not of uniform width. It is narrower at the posterior crus than at the anterior crus and not uniform in character in many adult ears (Bolz and Lim 1972). In early studies, von Békésy (1960) observed rocking movements of the footplate about 2 axes. More recently Hato et al. (2003) and Heiland et al. (1999) made observations with a laser Doppler vibrometer at multiple sites on the footplate and have shown that the stapes motion is complex, even at physiological levels (<120 dB). For simple physical reasons, such nonlinear behavior must occur at levels typical of gunfire (Price 1974). In effect, the footplate of the human stapes must radiate as something of a dipole or quadripole source and must be less effective than a simple piston moving linearly. We account for this loss in efficiency by using a smaller “effective footplate area”.

After the nonlinear solution for stapes displacement has been found, it then becomes the input for the linear cochlear calculation. For this calculation we use a fast method developed by Zweig et al. (1976). The cochlea is modeled as a 1-dimensional fluid-filled transmission line with exponentially tapered cross-sectional area and BM width. The motion is assumed to be linear—that is, positive feedback effects of the outer-hair cells giving rise to cochlear amplification at lower excitation levels are ignored. A linear WKB solution for the complex displacement transfer function as a function of driving frequency is obtained. This transfers frequency components of the stapes displacement with amplitude and phases given by a Fourier transform analysis of the stapes displacement time-waveform into magnitude and phases of components at 23 equally spaced locations on the BM (between .425 cm and 3.175 cm from the basal end). The resulting BM displacement histories are obtained by an inverse Fourier transform of these frequency components at each location.

Hazard within the cochlea is thought of as analogous to mechanical fatigue (i.e., the number of flexes and their amplitudes need to be monitored). Therefore, we calculate hazard at each of the 23 locations for which a displacement history was just determined by establishing the maximum upward displacement between successive zero-crossings, squaring the value (in microns) and summing it for the location. The result is in ARUs, which have been related to temporary and permanent hearing loss in experimental animals (Price 2003). A dose of more than 500 ARUs received within 1 day would be expected to produce permanent hearing loss.

6.2 Stepping Through the Program Calculation

We assume that the pressure history has been imported and has been written as a file with the .AHA extension. In it the waveform is given as an ASCII file with a TAB-delimited header, followed by pressure values in scientific notation. The header contains information about the recording such as sample rate, input location number, title, and various derived quantities.

- 1) Read the pressure-history waveform measured outside the head in the free field.
- 2) Multiply the SPL values by 3.126 (10 dB) to account for susceptibility of the 95th-percentile ear.
- 3) Set the variables appropriate to the assumed condition of the middle ear muscles (warned or elicited) for the following calculation.

- 4) Numerically integrate the set of 24 coupled second order differential equations governing the displacements and velocities of electroacoustic elements in the model of the outer and middle ear. The result is the predicted stapes displacement for the input waveform.

All equations are linear except for one that describes clipping in the motion of the stapes. The annular ligament supporting the stapes is modeled with a stiffness and a damping that is a nonlinear function of the stapes displacement. The integration between successive input waveform time samples is performed using the fourth-order Runge-Kutta method with adaptive step size control (Press et al. 1992). The step size control is based on step doubling and monitoring the percentage change in the velocity of a number of elements that couple to the nonlinear stapes element. The step size number continues doubling until the worst-case velocity percentage change is below a given tolerance limit. The step size number is then reduced by dividing by a given AdaptFactor that is typically 2.7. This reduction continues until a minimum number of steps is reached, typically 256. The peak-limited stapes displacement waveform is stored internally at the same time values as the input pressure waveforms.

- 5) The stapes displacement is used to drive the cochlear model. For the intracochlear calculations, the cochlea has been terminated in a matching impedance at the helicotrema (a type 2 cochlear model is calculated with a finite termination impedance). We obtain a linear WKB solution for the complex displacement transfer function as a function of driving frequency. This transfers frequency components of the stapes displacement with amplitude, and phases given by a Fourier transform analysis of the stapes displacement history into magnitude and phases of components at 23 locations on the BM. The resulting BM displacements are obtained by an inverse Fourier transform of these frequency components.

The cochlea is modeled as a 1-D fluid-filled transmission line with exponentially tapered cross-sectional area and BM width. The motion is assumed to be linear—that is, positive feed-back effects of the outer-hair cells giving rise to cochlear amplification, present at low excitation levels, are ignored because the forces operating at high levels simply overwhelm them and a linear solution is appropriate. Note—this linear procedure would not be possible if any part of the transmission path is nonlinear. In the calculation of stapes displacement in step 2, the cochlea is represented by a fixed resistive load impedance with a low-frequency impedance element describing the helicotrema. Typically, 23 equally spaced locations on the BM, between .425 and 3.175 cm from the base, are chosen for waveform

calculation at the same sampling rate as that of the input pressure waveform. All waveforms are stored as columns in a matrix with rows representing displacements of the stapes and cochlea at successive times as related to the input pressure history. This information can be plotted as an animated movie of cochlear motion as the pressure waveform is evolving in time. The solution involves a number of standard complex arithmetic calculations such as the complex square root and complex power function with a complex exponent.

- 6) The auditory hazard is calculated by first determining, for each of the 23 locations calculated, the successive maxima of the displacements of the BM occurring between 2 successive zero displacements. The loss model is one of mechanical fatigue. Only the upward flexes of the BM displacements are determined (critical tissue within the OC is in tension—the most likely condition for failure), the downward displacements are considered less damaging and are ignored. These peaks of upward displacement (in microns) are squared and summed as a representation of the total “dose” at each of the 23 locations. This number, ARUs, is reported for each impulse. This number, furthermore, is cumulative for multiple exposures within a day. A value of more than 500 ARUs has been correlated with the onset of permanent loss and is, therefore, the limit for occasional exposure.

6.3 Parameter Values and Differential Equations

The circuit shown in Fig. 13 is a ladder network with 24 meshes, each having a volume velocity i_k (for $k = 1$ to 24) that are analogous to currents in an electrical network. Volume displacements q_k in the meshes are obtained by time integration of the volume velocities i_k that are, in turn, obtained by time integration of the volume velocity derivatives di_k/dt . The network can be driven by acoustic pressure p in any mesh. The state of the ear can be given at any time by the set of i_k and q_k values.

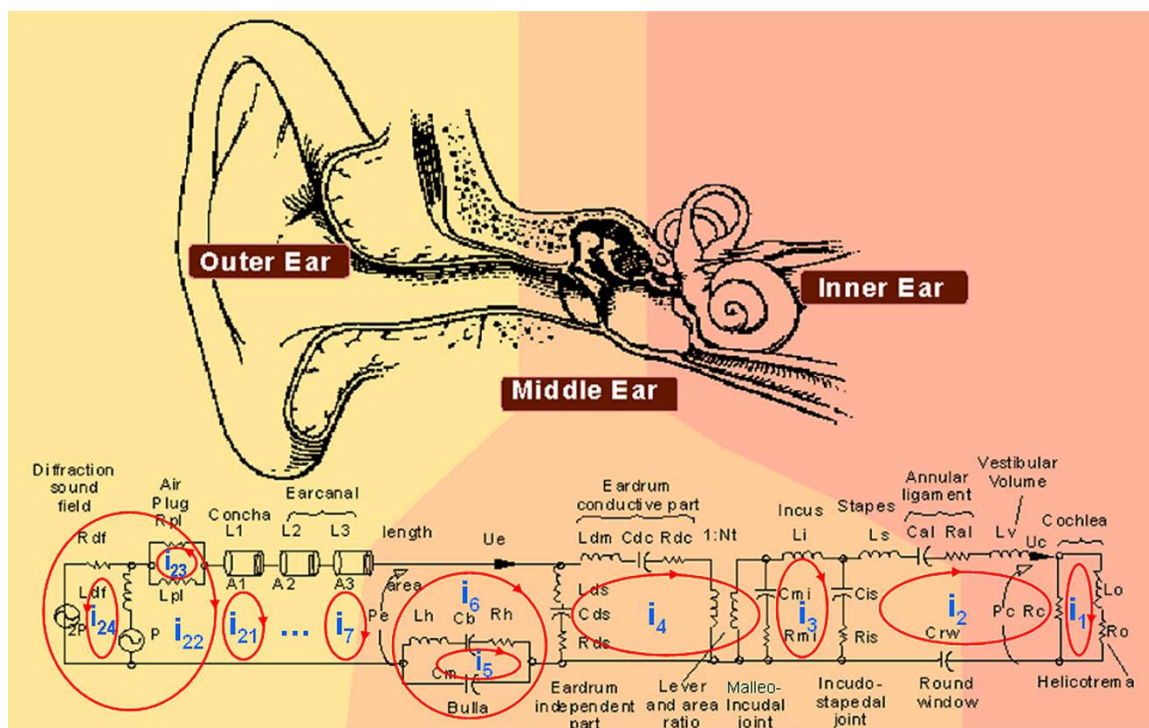


Fig. 13 The ladder network, corresponding ear sections, and in each section, the currents, in dynamically equivalent to volume velocities in the ear

The circuit element values and descriptions are given in Table 1.

Table 1 List of definitions and default values for all AHAAH calculation coefficients included in the file "man.coe"

Coefficient	Default value	Units	Description or purpose
Alphar	1	unitless	Induction field coupling, real part; always 1
Alphai	0	unitless	Imaginary part of Induction field coupling strength; always 0
Betar	2	unitless	Radiation field coupling, real part; (0 to 3); 2=normal incidence (90°), 1=grazing incidence (0°), 0=head-shadow incidence (270°)
Betai	0	unitless	Radiation field coupling, imaginary part ; usually 0
Rdf	1.29E-01	dyne.sec.cm ⁻⁵	Head diffraction radiation resistance;
Ldf	2.56E-05	g.cm ⁻⁴	Head diffraction inductive mass;
L1	2.215	cm	Length of cylindrical earcanal
L2	6.96E-01	cm	Length of exponential horn concha
S1	0.44	cm ²	Area of earcanal entrance; throat of exponential horn
S2	4.3	cm ²	Area of concha entrance; mouth of exponential horn
Lh	1.40E-02	g.cm ⁻⁴	Air-plug mass in narrow passages between tympanic cavity and remainder of middle-ear cavities.
Cb	5.10E-06	cm ⁵ .dyne ⁻¹	Compliance of the antrum and the pneumatic cells
Rh	91.85	dyne.sec.cm ⁻⁵	Loss in narrow passages between tympanic cavity and remainder of middle-ear cavities.;
Cm	3.50E-07	cm ⁵ .dyne ⁻¹	Compliance of middle-ear cavities; bulla volume in cm ³ /(rho * c ²)
Lds	4.60E-03	g.cm ⁻⁴	Nonconductive eardrum mass (assoc. with mode of vibration); Ad=0.55cm ²
Rds	1.147E+03	dyne.sec.cm ⁻⁵	Nonconductive eardrum loss (assoc. with mode of vibration) mechanical resistance(dyne/(cm/sec))/Ad ²
Cds	3.95E-07	cm ⁵ .dyne ⁻¹	Compliance of nonconductive part of eardrum
Ldm	2.20E-02	g.cm ⁻⁴	Mass of conductive part of eardrum and malleus for mode of vibration
Cdc	2.31E-06	cm ⁵ .dyne ⁻¹	Compliance of conductive part of eardrum and suspensory ligaments of ossicular chain
Rdc	60.6	dyne.sec.cm ⁻⁵	Loss of conductive part of eardrum and ossicles
Nt	20	unitless ratio	Turns ratio of transformer of middle ear = Astapes*Li/(Ad*Lm) Astapes= 0.021 cm ² stapes area
Rmi	8.39E+05	dyne.sec.cm ⁻⁵	Loss of the malleo-incudal joint;
Cmi	4.33E-10	cm ⁵ .dyne ⁻¹	Compliance of the malleo-incudal joint;
Li	2.44	g.cm ⁻⁴	Mass of incus;
Ris	4.75E+04	dyne.sec.cm ⁻⁵	Loss of the incudo-stapedial joint
Cis	4.57E-10	cm ⁵ .dyne ⁻¹	Compliance of the incudo-stapedial joint
Ls	2.44	g.cm ⁻⁴	mass of stapes
Lv	6.25	g.cm ⁻⁴	Mass of perilymph in vestibule between stapes and basal end of basilar membrane
Lo	52.4	g.cm ⁻⁴	Mass of perilymph in helicotrema

Coefficient	Default value	Units	Description or purpose
Ral	2.06E+05	dyne.sec.cm ⁻⁵	Resistance of annular ligament linear for stapes displacements < 10 microns
Rc	2.64E+06	dyne.sec.cm ⁻⁵	Resistance at base of cochlea
Ro	1.80E+05	dyne.sec.cm ⁻⁵	Resistance of perilymph in helicotrema
Cal	4.90E-10	cm ⁵ .dyne ⁻¹	Compliance of annular ligament; linear for stapes displacements < 10 microns
Crw	1.38E-08	cm ⁵ .dyne ⁻¹	Compliance of round-window
Astapes	2.10E-02	cm ²	Effective area of stapes footplate
Lgap	30	μm	Gapwidth of annular ligament
Eo	0.01	unitless	Equilibrium strain of annular ligament filaments
Eb	0.2	unitless	Breaking strain of annular ligament filaments
Ramp	6	unitless ratio	Ratio of resistance to stiffness of annular ligament at high loads
So	1.00E+09	dyne.cm ⁻³	Basilar membrane mechanical stiffness per unit area at base
Mo	0.0058	g.cm ⁻³	Effective mass of basilar membrane and vertically moving fluid, per unit area, at base of basilar membrane
Rvo	91.2	dyne.sec.cm ⁻³	Basilar membrane viscous-resistance per unit area at base
Bo	0.008	cm	Width of basilar membrane at base
Ao	0.0125	cm ²	Effective scala cross-section area = Sv*St/(Sv+St)
Fo	20000	Hz	Maximum audible frequency associated with motion at base of basilar membrane
Delo	0.03	unitless	Loss constant at base of basilar membrane full-width-at-half-maximum/characteristic freq
D1	0.666	cm	S(x)=So exp(-x/D1) stiffness decrement characteristic length D1=1/(2/Dc-1/D2)
D2	1	cm	M(x)=Mo exp(x/D2) mass increment characteristic length (D2=D4/2)
D3	1	cm	R(x)=Rvo exp(x/D3) resistance increment characteristic length (D3=D4/2)
D4	2	cm	B(x)=Bo exp(x/D4) basilar membrane width increment characteristic length
D5	2	cm	A(x)=Ao exp(-x/D5) Scala area decrement characteristic length (D5=D4)
Dc	0.8	cm	F(x)=Fo exp(-x/Dc) characteristic length for resonant frequency
Nw	2.0	unitless	number of wavelengths of the wave on the basilar membrane
Ca	0.5	unitless	Cochlear amplifier gain (from 0.1 to 10)
Bcoef	2	unitless	Bcoef stress fatigue power-law coefficient
XbApex	3.5	cm	Length of cochlea from base to apex
XbmFrom	0.425	cm	Starting distance from base of basilar membrane
XbmTo	3.175	cm	Ending distance from base of basilar membrane
XbmNo	23	unitless	Number of analysis locations on basilar membrane
SweightBase	1.0	unitless	Stress weighting at base of cochlea X=0
SweightApex	1.0	unitless	Stress weight at apex of cochlea X=Xbapex

Coefficient	Default value	Units	Description or purpose
Damage Threshold	0	cm	Damage Threshold, displacement threshold on basilar membrane at which damage begins
MemDelay	9.00E-03	seconds	Activation time of aural reflex relative to arrival of sound for unwarned ear is 9.0E-3 s; for the warned ear this is always set to -50.0E-3 s by the program
MemTimeConstant	1.17E-02	seconds	Rise-time constant after activation of aural reflex
MemMagK	12	unitless	Stiffness after divided by stiffness before activation of aural reflex
MemMagR	12	unitless	Loss after divided by loss before activation of aural reflex
AdaptFactor	2.5	unitless	Relaxation factor in auto-adaptive step-size algorithm in middle ear integrator
CochlearGainFactor	0.0724	unitless	WKB multiplicative factor (0.15 for WKBOrig) (0.025 for WKB taper)
WkbScalaBMwidthDecay	0.75	cm ⁻¹	WKB characteristic decay inverse-length based on tapering factors
CochlearModelType	2	nominal value	CochlearModelType: 3=WKB No Taper, 2=WKB Taper, 1=WKB Untapered
MakeXfrFile	0	nominal value	Store calculated transfer function: 1=Yes, 0=No, (not used)
PrintHazTable	1	nominal value	Store distances, frequency locations and hazards in cochlea: 1=Yes 0=No
SaveBMD	0	nominal value	Store basilar membrane displacement waveforms: 1=Yes 0=No (not used)
SaveSTD	0	nominal value	Store stapes displacement waveforms: 1=Yes 0=No (not used)
MultiGraph	0	nominal value	MultiGraph: 1=Yes 0=No (not used)
HornExtEar	1	nominal value	Choice of external ear geometry model: 1=Exponential Horn, 0=Three-cylinders
Tm3Piston	1	nominal value	Eardrum model: 1=Two pistons (three-piston model not used)
TerminateCochlea	0	nominal value	Cochlear termination choice: 1=infinite length, 0=finite length

Note: All values in this table are given as specific acoustic quantities. Ear protection property values in the man.coe file have been superseded by values in the "HPD Atten.txt" file. For additional details on the function of these parameters, see Price, G. R. and Kalb, J. T. (1991). "Insights into hazard from intense impulses from a mathematical model of the ear," J. Acoust. Soc. Am., 90, 219-227.

The values may be constant or else vary as a function of time, v_k or q_k as pressure levels rise and transmission becomes nonlinear. The acoustic transformer in the network can be removed by transforming the circuit elements to the right into primed values related to their original values and the transformer turns ratio N_t . In addition to the coefficient values provided in Table 1, physical constant values and addition term definitions are provided in Appendix A.

First, define the following pressures that are located at the indicated locations in the middle ear. The equations to be integrated are the following:

$$e_c = (i_2 - i_1)R'_c \quad \text{basal end of cochlea} \quad (1)$$

$$e_{is} = (i_3 - i_2)R'_{is} + (q_3 - q_2)K'_{is} \quad \text{incudo-stapedial joint} \quad (2)$$

$$e_{mi} = (i_4 - i_3)R'_{mi} + (q_4 - q_3)K'_{mi} \quad \text{malleolar-incudal joint} \quad (3)$$

$$e_{ds} = (i_6 - i_4)R_{ds} + (q_6 - q_4)K_{ds} \quad \text{eardrum shunt piston} \quad (4)$$

$$e_{dc} = (i_4)R_{dc} + (q_4)K_{dc} \quad \text{eardrum conductive piston} \quad (5)$$

$$e_{ma} = (q_6 - q_5)K_m \quad \text{mastoid volume} \quad (6)$$

In the k -th ear-canal volume-element the pressure is given by $e_{ec}[k]$ where $k = 6$ is the element closest to the eardrum and $k = 21$ is the element at the ear-canal entrance.

$$e_{ec}[k] = (q_{k+1} - q_k)K_{ec} \quad \text{for } k = 6, 7, 8 \dots 21 \quad (7)$$

Define the following intermediate pressures in the vicinity of the eardrum.

$$e_{Lec1} = e_{ec}[6] - e_{ds} - e_{ma} \quad \text{inertial pressure} \quad (8)$$

$$e_{LdsLdm} = e_{ds} - e_{dc} - e_{mi} \quad \text{sum of internal pressures on eardrum} \quad (9)$$

e_{Lec1} is the inertial pressure acting on the air mass in the ear-canal volume element which contacts the two pistons of the eardrum. e_{LdsLdm} is the sum of the inertial pressures acting on the two pistons of the eardrum. The pressure drop across the air-plug in the ear-canal entrance is e_{pl} .

$$e_{pl} = (i_{22} - i_{23})R_{pl} \quad \text{pressure drop} \quad (10)$$

e_{pl} is pressure drop across air plug in ear canal entrance.

$$e_{df} = (i_{24} - i_{22})R_{df} \quad \text{pressure drop} \quad (11)$$

e_{df} is the pressure drop across the resistive component of the diffraction sound field.

Rates of change in volume flow rate currents are given with inductor inertial mass equivalents:

$$\frac{di_1}{dt} = (e_c - i_1 R'_o)/L'_o \quad (12)$$

$$\frac{di_2}{dt} = (e_{is} - e_c[i_2 R'_{al} + q_2(K'_{al2} + K'_{rw})]) / (L'_s + L'_v) \quad (13)$$

$$\frac{di_3}{dt} = (e_{mi} - e_{is}) L'_i \quad (14)$$

$$L_{den}^2 = (L_{ds} + L_{dm})(L_{ds} + 0.5L_{ec}[1]) - L_{ds}^2 \quad (15)$$

$$\frac{di_4}{dt} = [e_{Lec1}L_{ds} + e_{LdsLdm}(L_{ds} + 0.5L_{ec}[1])]/L_{den}^2 \quad (16)$$

$$\frac{di_5}{dt} = [e_{ma} - (i_5 R_h + q_5 K_b)] / L_h \quad (17)$$

$$\frac{di_6}{dt} = [e_{Lec1}(L_{dm} + L_{ds}) + e_{LdsLdm}L_{ds}]/L_{den}^2 \quad (18)$$

$$\frac{di_k}{dt} = (e_{ec}[k] - e_{ec}[k-1]) / L_{ec}[k-5] \quad (19)$$

$$\frac{di_{22}}{dt} = (\beta_r p_f + e_{df} - e_{pl} - e_{ec}[21]) / (0.5L_{ec}[17]) \quad (20)$$

$$\frac{di_{23}}{dt} = e_{pl} / L_{pl} \quad (21)$$

$$\frac{di_{24}}{dt} = [(\alpha_r - \beta_r)p_f - e_{df}] / L_{df} \quad (22)$$

Details of the volume elements of the ear canal are shown in Fig. 14.

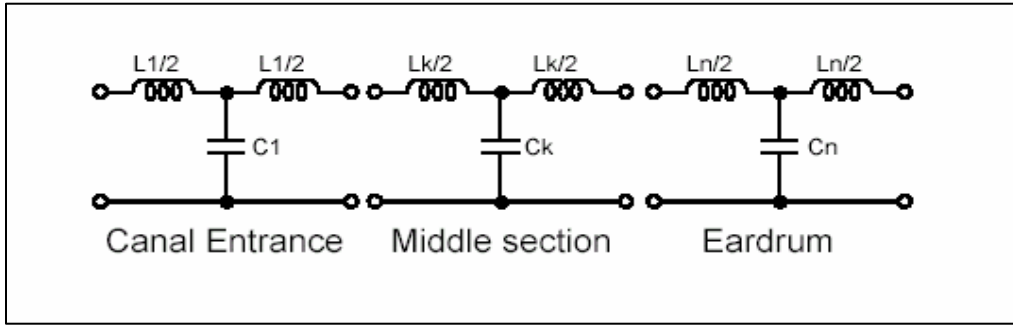


Fig. 14 Details of volume element representation in ear canal

A **horn-cylinder model** is used to simulate the concha and the ear canal. The ear canal is represented by a cylinder with cross section area, S_1 , and length, L_1 . Propagation through the ear canal is analyzed in 16 sections of the cylinder.

$$L_{tot} = 1 \quad \text{Total length of ear canal (cm)} \quad (23)$$

$$N_s = 16 \quad \text{Number of ear canal sections} \quad (24)$$

$$\Delta l = L_{tot} / N_s \quad \text{Length of each ear canal section} \quad (25)$$

$$x = k\Delta l \quad \text{Distance from eardrum (cm) for } k=1, 2, \dots, N_s \quad (26)$$

$$V(x) \text{ (cm)} \quad \text{Volume of ear canal section} \quad (27)$$

$$A(x) = V(x)/\Delta l \quad \text{Effective cross section of ear canal section (cm}^3\text{)} \quad (28)$$

$$K_e(k) = \rho_0 c^2 / V(x) \quad \text{Acoustic compliance of ear canal section} \quad (29)$$

$$L_e(k) = \frac{1}{2} \rho_0 \Delta l / A(x)$$

$$L_e(k) = \frac{1}{2} \rho_0 \Delta l^2 / V(x) \quad \text{Acoustic mass of each half of ear canal section} \quad (30)$$

The concha is represented by an exponential horn with throat area, S_1 , and mouth area, S_2 , and length, L_2 .

$$L_{tot} = L_1 + L_2 \quad \text{Total length from horn mouth to eardrum} \quad (31)$$

$$m = \ln(S_2/S_1)/L_2 \quad \text{Exponential horn flare factor} \quad (32)$$

$$V(x) = S_1 \Delta l \quad 0 \leq x \leq L_1 - \Delta l \quad (33)$$

$$V(x) = S_1(L_1 - x) + S_1(e^{m(x+\Delta l-L_1)} - 1)/m \quad L_1 - \Delta l < x < L_1$$

$$V(x) = S_1(e^{m(x+\Delta l-L_1)} - e^{m(x-L_1)})/m \quad L_1 \leq x \leq L_{tot} - \Delta l$$

Eardrum dynamics are described with a three-cylinder model - the eardrum cylinder area, S_1 , and length, L_1 , the outer ear canal cylinder, S_2 , and length, L_2 , and a concha cylinder, S_3 , and length, L_3 .

$$L_{tot} = L_1 + L_2 + L_3 \quad (34)$$

$$V(x) = S_1 \Delta l \quad 0 \leq x \leq L_1 - \Delta l \quad (35)$$

$$V(x) = S_1(L_1 - x) + S_2(x - \Delta l - L_1) \quad L_1 - \Delta l < x < L_1$$

$$V(x) = S_2 \Delta l \quad L_1 \leq x \leq L_1 + L_2 - \Delta l$$

$$V(x) = S_2(L_1 + L_2 - x) + S_3(x + \Delta l - L_1 - L_2) \quad L_1 + L_2 - \Delta l < x < L_1 + L_2$$

$$V(x) = S_3 \Delta l \quad L_1 + L_2 \leq x \leq L_1 + L_2 + L_3 - \Delta l$$

A general cross section right-cone-frustum model is applied as an array of $N+1$ cross sectional areas, $\{A_0, A_1, A_2, \dots, A_N\}$, measured at locations $\{0, \Delta l, 2\Delta l, \dots, N\Delta l\}$, where area A_0 is measured at the eardrum location $x = 0$, and A_N is measured at the canal-concha entrance at a distance $x = L_{tot}$ from the eardrum. The volume of the cone-frustum which begins at $x_k = k\Delta l$ with area A_k and ends at

$x_{k+1} = (k+1)\Delta l$ with area A_{k+1} is:

$$V(x_k) = \frac{(A_k + A_k^{1/2} A_{k+1}^{1/2} + A_{k+1})}{3} \Delta l \quad \text{for } 0 \leq k \leq N_s - 1 \quad (36)$$

Annular ligament compliance model

The annular ligament, which surrounds the footplate of the stapes at the entrance of the cochlea, is known to be a primary contributor to the cochlear input impedance (Lynch 1982). It is highly compliant for small movements about equilibrium, which is characteristic of normal listening levels. For larger forces due to higher SPLs, aural reflex rotations or imbalance in static pressures in fluid and air filled chambers, it reaches a displacement limit that is on the order of the width of the annular space, L_{gap} . In a simplified analysis of elastic properties of the ligament, Lynch assumed the material to be homogeneous, isotropic, relatively incompressible, and confined to the annular space. He found the shear modulus of the material to be 2–4 orders of magnitude lower than values for other ligaments. He concluded that the fibrous structure of the ligament would tend to make its elastic properties anisotropic and that the mechanically significant components of the ligament may not be uniformly distributed or completely confined. Bolz and Lim (1972) studied the annular ligament in several species and found that in adult animals, the structure of the ligament matched Lynch's characterization as anisotropic. Based on these conclusions, the following nonlinear "hardening" ligament model was developed and is shown in Fig. 15.

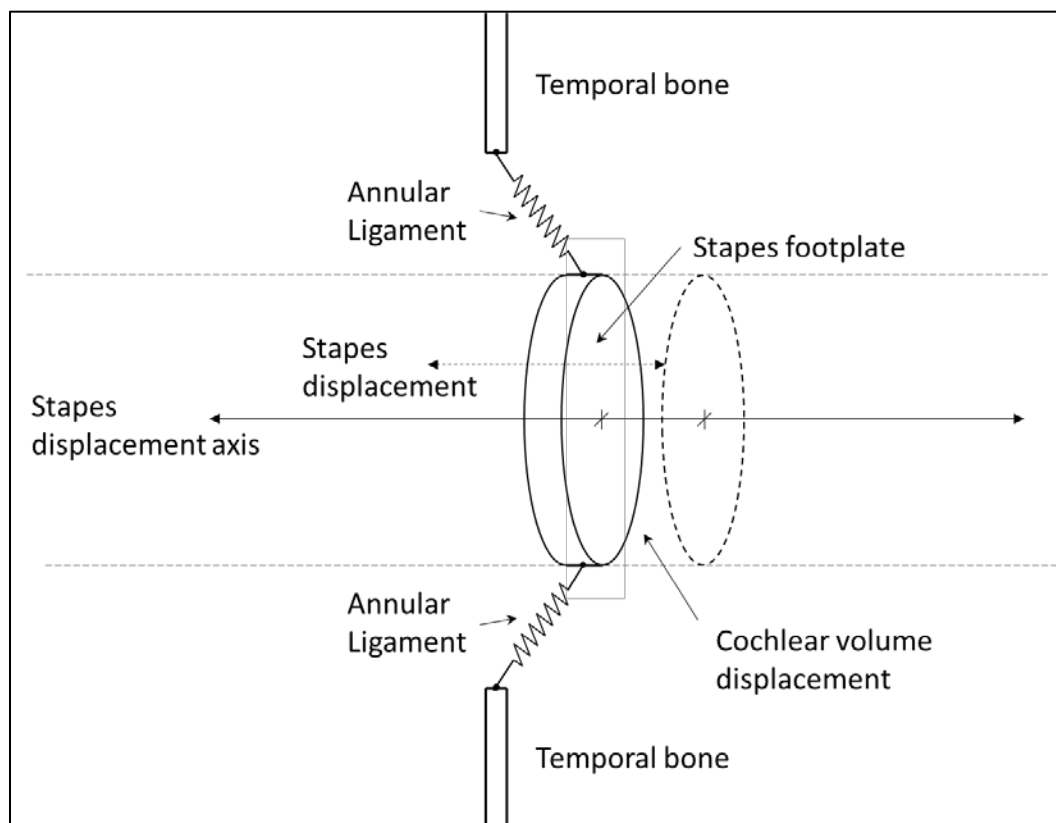


Fig. 15 Annular ligament shown as one of N standard springs

Figure 15 shows only 2 springs. All N springs are distributed around the stapes, in a plane perpendicular to the direction of stapes movement. Each spring contributes an equal force opposing lateral stapes movement.

The constitutive elastic properties of each spring as would be measured on a linear elongation apparatus are assumed to have a “tangent elasticity characteristic” (Broch 1964). Such a model describes a Cellophane “shatter”-type material that is frangible rather than plastic (i.e., it remains intact under increasing loading up to a breaking-point at a limiting displacement, d). The strain in the material at breaking is assumed to be E_b , which is given a value of 0.20 typical for biologic materials. Also, the springs are assumed not to be relaxed but mounted between their hinges with a “loaded” strain E_o equal to 0.01, which produces an equivalent tension, T_o , in the annular ligament, at zero stapes displacement, of $2.67E+01$ dynes. The expression for the restoring force acting on the stapes footplate for a purely translational stapes displacement of x is

$$F(z) = \left[\frac{T_o z}{\sqrt{L_o^2 + z^2}} + Kz - \frac{Kz}{\sqrt{1 + \left(\frac{z}{L_o}\right)^2}} \right] \tan\left(\frac{\pi z}{2x_{max}}\right). \quad (37)$$

In Eq. 15, L_o is the initial annular ligament length at zero stapes displacement, K is the stapes spring constant, and x_{max} is the effective maximum stapes displacement allowed in AHAAH.

This expression reduces to a linear expression for small displacements with the observed small-displacement spring constant, K_{al} , corresponding to a compliance given by $C_{al} = 1/K_{al}$. For large forces, the “Hookes-law” stiffness value K_{al} , increases by a stiffness amplification factor K_{amp} . Since the viscous properties of ligaments have not been measured at audio frequencies, a further assumption was made that the material resistance increased from its small displacement value R_{al} in direct proportion to the stiffness increase. This proportion is adjusted by a multiplicative amplification factor $R_{amp} = 6$. This has the effect of dissipating the energy stored in the system at very high intensities (reducing ringing) and in a physical sense is equivalent to the proposition that when driven very hard, the middle ear vibrates in modes that are not part of the normal conductive path.

As a further refinement for purpose of stability in the numerical analysis a displacement was chosen arbitrarily close to the breaking point for which the restoring force was truncated and did not increase with further increases in displacement. This prevented force reversals for displacements beyond the

breaking point that occur in the tentative steps of the auto-adaptive integration procedure.

The mathematical process of solving the given equations is implemented in Delphi (Embarcadero Technologies, Inc.) computed code. The source code for this process is included in Appendix B.

7. Conclusion

We have shown AHAAH is a quantitative, physical, dynamic model of auditory system response to intense, high-pressure, impulsive waveforms. We intentionally created a physical dynamic model for the evaluation of hearing damage from impulsive sounds because the characteristic of impulsive waveforms can not be described by any single parameter, or even any combination a few waveform parameters, and we needed to maximize the possibility that the assessment process would describe, as closely as possible, the damage resulting from exposure to any possible time-dependent impulsive waveform. AHAAH performs calculations detailing the step-by-step transport of waveforms from the free-field to the displacements produced in the basilar membrane where mechanical damage produces hearing loss. AHAAH was developed from existing research results describing auditory system dynamics and from available experimental results quantifying the auditory system damage caused by exposure to high-pressure, impulsive waveforms. However, we do not rule out the possibility that future research might provide improved understandings and descriptions of auditory system behavior. The step-by-step calculation process has been described to provide the opportunity for further research measurements to be applied to further validate, or improve, the overall performance of AHAAH. Today, the AHAAH model can be used to assess the hazard of exposure to impulsive sounds. Use of the model has been described by Binseel et al. (2009), with model updates described by Fedele et al. (2013). We hope that the scientific process will continue, AHAAH will continue to be tested, compared against further valid experimental procedures, and further validated and improved. We hope AHAAH, including any improvements, will provide the accurate hearing hazard predictions and associated materiel design guidance needed to keep protect hearing and ensure effective performance of Soldiers, military personnel, and all people.

8. References

- ANSI/ASA S3.44-1996 (R2006). Determination of occupational noise exposure and estimation of noise-induced hearing impairment. Melville (NY): Acoustical Society of America; 2006.
- ANSI/ASA S12.42-2010. Methods for the measurement of insertion loss of hearing protection devices in continuous or impulsive noise using microphone-in-real-ear or acoustic test fixture procedures. Washington (DC): American National Standards Institute; 2010.
- ANSI S12.6-1997. Methods for measuring the real-ear attenuation of hearing protectors. Washington (DC): American National Standards Institute; 1997.
- Bauer BB. On the equivalent circuit of a plane wave confronting an acoustical device. *J Acoust Soc Am*. 1967;42(5):1095–1097.
- Berger, Elliot H. Preferred methods for measuring hearing protector attenuation. In *INTER-NOISE and NOISE-CON Congress and Conference Proceedings*, vol. 2005, no. 3, pp. 4432-4441. Institute of Noise Control Engineering, 2005.
- Berger E, Kieper RW. Hearing protection: Surpassing the limits to attenuation by bone-conduction pathways. *J Acoust Soc Am*. 2003;114:1955–1967.
- Binseel M, Kalb J, Price GR. Using the Auditory Hazard Analysis Algorithm for Humans (AHAH) software, beta release W93e. Aberdeen Proving Ground (MD): Army Research Laboratory (US); 2009. Report No.: ARL-TR-4987.
- Bolz EA, Lim DJ. Morphology of the stapediovestibular joint. *Acta Oto-Laryngol*. 1972;73(1):10–17.
- Brasher PF, Coles RRA, Elwood MA, Ferres HM. Middle-ear muscle activity and temporary threshold shift. *Int Audiol*. 1969;8(4):579–584.
- Broch J. Random vibration of some non-linear systems. *Bruel & Kjaer Technical Review*. 1964;3; Naerum, Denmark.
- Broch JT. A theory of noise induced hearing damage. *Proceedings of the 97th meeting of the Acoustical Society of America*, 42; 1979; Cambridge, MA.
- Buck K. Performance of different types of hearing protectors undergoing high-level impulse noise. *Int J Occup Safety and Ergonom*. 2009;15(2):222–240.

- Coles RRA, Garinther GR, Hodge DC, Rice CG. Criteria for assessing hearing damage risk from impulse-noise exposure. Aberdeen Proving Ground (MD): Army Human Engineering Laboratories (US); 1967. Report No.: Technical Memorandum 13-67.
- Coles RRA, Garinther GR, Hodge DC, Rice CG. Hazardous exposure to impulse noise. *J Acoust Soc Am*. 1968;43(2):336–343.
- Dallos P. Dynamic of the acoustic reflex: phenomenological aspects. *J Acoust Soc Am*. 1964;36(11):2175–2183.
- Dancer A. Proposal for a new damage risk criterion. In: Report from NATO Research Study Group RSG.29 (Panel 8 – AC/243) Reconsideration of effects of impulse noise, TNO-Report TM-00-I008 (second meeting); 2000; Soesterberg (Netherlands). 11-15.
- Dancer A. The LAeq8 an effective DRC for weapon noises. NIOSH/NHCA Impulsive noise: A NORA Hearing Loss Team Best Practice Workshop; Cincinnati, OH. National Institute for Occupational Safety and Health; [accessed 2003] <http://www.cdc.gov/niosh/topics/noise/research/impulse presentations.html>.
- Djupestrand G. Middle ear muscle reflexes elicited by acoustic and nonacoustic stimulation. *Acta Oto-Laryngol, Suppl*. 1964;188:287–292.
- Djupestrand G. Electromyography of the tympanic muscles in man. *Intern Audiol*. 1965;4:34–41.
- Fedele, Paul D., Mary S. Binseel, Joel T. Klab, and G. Richard Price. Using the Auditory Hazard Assessment Algorithm for Humans (AHAH) With Hearing Protection Software, Release MIL-STD-1474E. Aberdeen Proving Ground (MD): Army Research Laboratory (US); 2013. Report No.: ARL-TR-6748.
- Fedele P, Kalb J. Level-dependent nonlinear hearing protector model in the Auditory Hazard Assessment Algorithm for Humans. Aberdeen Proving Ground (MD): Army Research Laboratory (US); 2015. Report No.: ARL-TR-7271.
- Flamme GA, Deiters KK, Tasko SM, Ahroon WA. Prevalence of acoustic reflexes in the United States. *J Acoust Soc Am*. 2015;138:1831–32.
- Greenwood D. A cochlear frequency-position function for several species – 29 years later. *J Acoust Soc Am*. 1990;87:2592–2605.
- Guinan JJ, Peake WT. Middle ear characteristics of anesthetized cats. *J Acoust Soc Am*. 1967;41:1237–1261.

- Gyo K, Aritomo H, Goode R. Measurement of the ossicular vibration ratio in human temporal bones by use of a video measuring system. *Acta Otolaryngol.* 1987;103:87–95.
- Hamernik RP, Ahroon WA, Patterson JH, Jr. Threshold recovery functions following impulse noise trauma. *J Acoust Soc Am.* 1988;84:941–950.
- Hamernik RP, Qiu W, Davis B. Cochlear toughening, protection, and potentiation of noise-induced trauma by non-Gaussian noise. *J Acoust Soc Am.* 2003;113:969–976.
- Hato N, Stenfeldt S, Goode RL. Three-dimensional stapes footplate motion in human temporal bones. *Audiol Neurotol.* 2003;8:140–152.
- Heiland KE, Goode RL, Asai M, Huber AM. A human temporal bone study of stapes footplate movement. *Am J Otol.* 1999;20(1):81–86.
- Henderson D. Individual susceptibility to noise-induced hearing loss: A review. *J Acoust Soc Am.* 2006;119–3267 A
- Henderson D, Hamernik RP. Impulse noise: critical review. *J Acoust Soc Am.* 1986;80:569–584.
- Henderson D, Subramaniam M, Boettcher FA. Individual susceptibility to noise-induced hearing loss: An old topic revisited. *Ear & Hearing.* 1993;14:152–168.
- Hirsh IJ, Ward WD. Recovery of auditory threshold after strong acoustic stimulation. *J Acoust Soc Am.* 1952;24:131–141.
- Hodge DC, McCommons BM. Reliability of TTS from impulse-noise exposure. *J Acoust Soc Am.* 1966;40:839–846.
- Hodge DC, McCommons BM, Blackmer RF. Reliability of temporary threshold shifts caused by repeated impulse-noise exposures. Aberdeen Proving Ground (MD): Army Human Engineering Laboratories (US); 1965. Report No.: Tech. Memo. 3-65.
- ISO 1999. Acoustics – Determination of occupational noise exposure and estimation of noise-induced hearing impairment. Geneva, Switzerland: International Organization for Standardization; 1990.
- Johnson DL. Blast overpressure studies. Ft. Rucker (AL): Army Aeromedical Research Laboratory (US); 1998. Report No.: USAARL Contract Report No. CR-98-03.

- Johnson DL, Patterson JH. Rating of hearing protector performance for impulse noise. Ft. Rucker (AL): Army Aeromedical Research Laboratory (US); 1993. Report No.: USAARL 93-20.
- Kalb, Joel T. An electroacoustic hearing protector simulator that accurately predicts pressure levels in the ear based on standard performance metrics. Aberdeen Proving Ground (MD): Army Research Laboratory (US); 2013. Report No.: ARL-TR-6562.
- Kalb JT, Price GR. Mathematical model of the ear's response to weapons impulses. In: Proceedings of the Third Conference on Weapon Launch Noise Blast Overpressure. Aberdeen Proving Ground (MD): Army Ballistics Research Laboratory (US); 1987. Report No: ARL-RP-0521.
- Kalb J. A hearing protector model for predicting impulsive noise hazard. J Acoust Soc Am. 2010;127:1879 (A)
- Kalb JT. A hearing protector model for predicting impulsive noise hazard. Proceedings of POMA and Program of 159th ASA/NOISE-CON meeting; 2010 Apr; Baltimore, MD.
- Kringlebotn M, Gunderson T. Frequency characteristics of the middle ear. J Acoust Soc Am. 1985;77:159–164
- Kryter KD. The effects of noise on man. New York (NY): Academic Press; 1970.
- Kujawa SG, Liberman MC. Noise-induced and age-related hearing loss interactions. J Acoust Soc Am. 2006;119:3268A.
- Kujawa SG, Liberman MC. Adding insult to injury: cochlear nerve degeneration after “temporary” noise-induced hearing loss. J Neuroscience. 2009;29:14077–14085.
- Lauxman M, Eiber A, Haag F, Ihrle, S. Nonlinear stiffness characteristics of the annular ligament. J Acoust Soc Am. 2014;136:1756–1767.
- Loeb M, Fletcher JL. Impulse duration and temporary threshold shift. J Acoust Soc Am. 1968;44:1524–1528.
- Luz GA, Hodge DC. The recovery from impulse noise-induced TTS in monkeys and men: A descriptive model. J Acoust Soc Am. 1971;49:1770–1777.
- Lynch III, TJ, Nedzelnitsky V, Peake WT. Input impedance of the cochlea in cat. J Acoust Soc Am. 1982;72(1):108–130.
- Marshall L, Brandt JF, Marston LE. Anticipatory middle ear reflex activity from noisy toys. J Speech Hear Disord. 1975;40:320–326.

- Marshall L, Lapsley Miller JA, Heller LM. Can oto-acoustic emissions indicate individual susceptibility to noise-induced hearing loss in individual ears? *J Acoust Soc Am*. 2006;119:3267A
- Mehrghardt S, Mellert V. Transformation characteristics of the external human ear. *J Acoust Soc Am*. 1977;61:1567–1576.
- Miller JD. Audibility curve in the chinchilla. *J Acoust Soc Am*. 1970;48:513–523.
- Murphy WJ, Kahn A, Shaw PB. An analysis of the blast overpressure study data comparing three exposure criteria. Cincinnati (OH): Department of Health and Human Services, NIOSH (US); 2009. Report No.: Rept #EPHB 309-05h.
- Murphy, William J., and Chucuri A. Kardous. A case for using a-weighted equivalent energy as a damage risk criterion. Cincinnati (OH): National Institute for Occupational Safety and Health; 2012. Report No: Rept #EPHB Report No 350-11a.
- NATO RSG6/PANEL8 The effects of impulse noise. Document AC/243/(PANEL8/RSG.6)D/9, NATO, 1110 Brussels, 1987, 33pp.
- Peters L, Garinther GR. The effects of speech intelligibility on crew performance in an M1A1 tank simulator. Aberdeen Proving Ground (MD): Army Human Engineering Laboratories (US); 1990. Report No.: Technical Memorandum 11-90.
- Pfander F, in collaboration with Bongartz H, Brinkmann H, *Das Knalltrauma*, Springer Verlag, Berlin, 1975.
- Pierson LL, Price GR, Kalb JT, Mundis PA. Comparison of impulse noise effects generated by two rifle muzzles. *J Acoust Soc Am*. 1995;97:3344.
- Press, William H., Saul A. Teukolsky, William T. Vetterling, and Brian P. Flannery. *Numerical recipes in C*. 1992. Cambridge (UK): Cambridge University; 1992.
- Price GR, Kalb JT. Proposal for standard method for measuring and evaluating noise hazard. Proceedings of the NATO Research Study Group 29 on the effects of impulse noise; 1998 Oct; Soesterburg, The Netherlands.
- Price GR, Kalb JT. Auditory hazard from airbag noise exposure. *J Acoust Soc Am*. 1999;106:2629–2637.
- Price GR, Kalb JT, Garinther GR. Toward a measure of auditory handicap in the Army. *Ann Otol Rhinol Laryngol*. 1989;98:42–52.

- Price, Richard G., Joel T. Kalb, and Charles R. Jokel. "brief critical examination of the article: "impulse noise injury prediction based on the cochlear energy" by Zagadou, Chan, Ho and Shelly." *Hearing research* 350 (2017): 43-44.
- Price, G. Richard, Joel T. Kalb, and Charles R. Jokel. *Critical Examination of the Article Impulse Noise Injury Prediction Based on the Cochlear Energy by Zagadou, Chan, Ho, and Shelly*; 2017. Aberdeen Proving Ground (MD): Army Research Laboratory. No. ARL-TR-7958.
- Price GR, Pierson LL, Kalb JT, Mundis P. Validating a mathematical model of noise hazard with varying numbers of rounds and peak pressures produced by a rifle. *J Acoust Soc Am*. 1995;97:3343.
- Price GR, Wansack S. Hazard from an intense mid-range impulse. *J Acoust Soc Am*. 1989;86:2185–2191.
- Price GR. Functional changes in the ear produced by high intensity sound. I. 5.0-kHz stimulation. *J Acoust Soc Am*. 1968;44:1541–1545.
- Price GR. Functional changes in the ear produced by high intensity sound. II. 500-Hz stimulation. *J Acoust Soc Am*. 1972;51:552–558.
- Price GR. Loss and recovery processes operative at the level of the cochlear microphonic during intermittent stimulation. *J Acoust Soc Am*. 1974;56:183–189.
- Price GR. An upper limit to stapes displacement: Implications for hearing loss. *J Acoust Soc Am*. 1974;56:195–197.
- Price GR. Effect of interrupting recovery on loss in cochlear microphonic sensitivity. *J Acoust Soc Am*. 1976;59:709–712.
- Price GR. Implications of a critical level in the ear for the assessment of noise hazard at high intensities. *J Acoust Soc Am*. 1981;69:171–177.
- Price GR. Relative hazard of weapons impulses. *J Acoust Soc Am*. 1983;73:556–566.
- Price GR. Middle ear muscle effects during gunfire exposures. *J Acoust Soc Am*. 1991;89:1865.
- Price GR. *Impulse noise and the cat cochlea*. Aberdeen Proving Ground (MD): US Army Research Laboratory; 2003 [accessed 2018 Mar 27]. <http://www.arl.army.mil/www/default.cfm?page=352>.

- Price GR. A new method for rating hazard from intense sounds: Implications for hearing protection, speech intelligibility and situation awareness. NATO RTO-MP-HFM-123 symposium “New directions for improving audio effectiveness”, 14 Apr 2005. Brussels, Belgium.
- Price GR. Insights into hazard from airbag noise gained through the AHAAH model. Paper 2005-01-2397, SAE 2005 Transactions Journal of Passenger Cars: Mechanical Systems, Book V114-6. 2006.
- Price GR. Predicting mechanical damage to the organ of Corti. Hearing Res. 2007 Apr;226(1-2):5-13.
- Price GR. Validation of the auditory hazard assessment algorithm for the human with impulse noise data. J Acoust Soc Am. 2007;122:2786–2802.
- Price GR. Critique of an analysis of the blast overpressure study data comparing three exposure criteria by Murphy, Kahn, and Shaw. Aberdeen Proving Ground (MD): Army Research Laboratory (US); 2010a. Report No.: ARL-CR-657.
- Price GR. Susceptibility to intense impulse noise: evidence from the Albuquerque dataset. Program of 159th ASA/NOISE-CON meeting; Apr 2010; Baltimore (MD). J Acoust Soc Am. 2010b;127:1746.
- Price GR. Impulse noise hazard: from theoretical understanding to engineering solutions. Noise Con Eng J. 2012;60(3):301–312.
- Royster JD, Berger EH, Merry CJ, Nixon CW, Franks JR, Behar A, Casali JG, Dixon-Ernst C, Kieper RW, Mozo BT, Ohlin D, Royster LH. Development of a new standard laboratory protocol for estimating the field attenuation of hearing protection devices. Part I: Research of Working Group 11, Accredited Standards Committee S12, Noise. J Acoust Soc Am. 1996;99:1506–1526.
- SAE Standards. J2531: Impulse noise from automotive inflatable devices. SAE International; 2003.
- Schröter J. Messung der Schalldämmung von Gehörschützern mit einem physikalischen Verfahren (Kunstkopfmethode) (Assessment of Hearing Protector Attenuation by a Physical Method [Dummy-Head Measurement]), Wirtschaftsverlag NW, Bremerhaven, Fed. Rep. of Germany, 1983.
- Schröter J, Pössl C. The use of acoustical test fixtures for the measurement of hearing protector attenuation. Part II: Modeling the external ear, simulating bone conduction, and comparing test fixture and real-ear data. J Acoust Soc Am. 1986;80:505–527.

- Shaw EAG, Thiessen GJ. Acoustics of circumaural earphones. *J Acoust Soc Am*. 1962;34:1233–1246.
- Shaw EAG, Thiessen GJ. Improved cushion for ear defenders. *J Acoust Soc Am*. 1958;30:24–36.
- Sheffield B, Brungart D, Blank A. The effects of hearing impairment on fire team performance in dismounted combat. Proceedings of the Human Factors and Ergonomics Society Annual Meeting; 2016 Sep; Washington, DC. Los Angeles (CA): SAGE Publications.
- Sommer HC, Nixon CW. Primary components of simulated air bag noise and their relative effects on human hearing. Final Report, DOT Contract Number IA-0-1-2160, 1973.
- Smootenburg GF. Damage risk criteria for impulse noise. In: Hamernik RP, Henderson DH, Salvi R, editors. New perspectives on noise-induced hearing loss. New York (NY): Raven Press; 1982. p. 471–490.
- Summerfield A, Florig A, Wheeler D. Is there a suitable industrial test of susceptibility to noise-induced hearing loss? *Noise Control*. 1958;56:40–46.
- Tempel BL, Street VA, Kujawa SG. Searching the whole genome to identify genes contributing to noise resistance in inbred mouse strains. *J Acoust Soc Am*. 2006;119:3267A
- Vause NC, LaRue AA. Creating our own casualties – Auditory effects of anti-tank weapons fire without hearing protection – A clinical case study. Proceedings of the International Military Noise Conference; 2001 Apr 24–26; Baltimore, MD.
- Von Békésy G. Zur physik des mittelhöres and über des hören bei fehlerhaftem trommelfell. *Akust. Zeits.*, 1, 13-23. In: Experiments in hearing. New York (NY): McGraw-Hill; 1960, 1936.
- Von Békésy G. In: Wever EG, editor. Experiments in hearing. New York (NY): McGraw-Hill; 1960.
- Ward WD. Susceptibility to auditory fatigue. In: Neff WD, editor. Advances in Sensory Physiology. Vol 3. New York (NY): Academic Press; 1967.
- Ward WD. Effect of temporal spacing on temporary threshold shift from impulses. *J Acoust Soc Am*. 1962;34:1230–1232.
- Ward WD, Glorig A, Sklar D.L. Temporary threshold shift from octave band noise: Applications to damage-risk criteria. *J Acoust Soc Am*. 1959;31:522–528

- Yonovitz A. Classical conditioning of the stapedius muscle. *Acta Oto-Laryngol.* 1976;82:11–15.
- Zagadou B, Chan P, Ho K, Shelley D. Impulse noise injury prediction based on the cochlear energy. *Hearing Res.* 2016;342:23–38.
- Zhang X, Gan RZ. Dynamic properties of human stapedial annular ligament measured with frequency-temperature superposition. *J Biomech Eng.* 2014;136(8):doi: 10.1115/14027668.
- Zweig G, Lipes R, Pierce JR. The cochlear compromise. *J Acoust Soc Am.* 1976;59(4):975.
- Zwislocki J. Ear protectors. In: Harris CM, editor. *Handbook of noise control*. New York (NY): McGraw-Hill; 1957; p. 1–27.

Appendix A. Physical Constant Definitions

$\rho_w = 1 (g/cm^3)$	Density of water
$f_0 = 20,000 (Hz)$ basilar membrane	Maximum resonant frequency at base of
$\omega_0 = 2\pi f_0 (sec^{-1})$	Maximum resonant angular frequency
$f (Hz)$	Excitation frequency
$\omega = 2\pi f (sec^{-1})$	Excitation angular frequency
$a_0 = 1.2E - 2 (cm^2)$	Effective scala cross-sectional area at base
$b_0 = 8.0E - 3 (cm)$	BM width at base
$S_0 = 1.0E + 9 (dyne/cm^3)$	BM stiffness at base
$m_0 = S_0/\sqrt{\omega_0} (g/cm^2)$ area at base	BM mass plus vertically moving fluid mass per unit
$X_{bm} (cm)$	Distance along the BM from base
$D_C = 0.8 (cm)$ distance	BM resonant frequency decrease characteristic
$D_1 = 0.666 (cm)$	BM stiffness decrease characteristic distance;
$D_1 = 1/(2/D_C - 1/D_2)$	Distance factor
$D_2 = 1.0 (cm)$ $D_4/2$	BM mass increase characteristic distance; $D_2 =$
$D_3 = 1.0 (cm)$ $D_2 = D_4/2$	BM resistance increase characteristic distance;
$D_4 = 2.0 (cm)$	BM width increase characteristic distance
$D_5 = 2.0 (cm)$ D_4	Scalae area decrease characteristic distance; $D_5 =$
$c_1 = Cgf\sqrt{\rho_w/m_0b_0a_0} a_{stapes}e^{-0.75X_{bm}/D_2}$ amplitude term	Frequency-independent
$N4 = \sqrt{\rho_wb_0/m_0a_0} 2D_1D_2/(D_1 + D_2)$ propagating on BM	Number of waves
$\delta_0 = 0.03$	Loss constant at base of BM
$c_a = 0.5$	Cochlear amplifier gain
$\omega_r = \omega_0 e^{-X_{bm}/D_C}$	Resonant frequency at distance X_{bm}
$\bar{\gamma} = \sqrt{1 - i\delta_0\omega_0/\omega}$	

$$\bar{z}_0 = \frac{\omega}{\omega_0} - i \frac{\delta}{2}$$

$$\bar{z}_x = \frac{\omega}{\omega_r} - i \frac{\delta}{2}$$

$$D(x, \omega) = c_1 \left(\frac{\omega}{\omega_r} \right)^{1/2} \left(\frac{i\omega/\omega_r}{\sqrt{1-\bar{z}_x^2}} \right) \left(\frac{\sqrt{1-\bar{z}_0^2}}{\sqrt{1-\bar{z}_x^2}} \right)^{1/2} \left(\frac{i\bar{z}_0 + \sqrt{1-\bar{z}_0^2}}{i\bar{z}_x + \sqrt{1-\bar{z}_x^2}} \right)^{N4/\gamma}$$

$$\Phi(x) = \left(\frac{i\bar{z}_0 + \sqrt{1-\bar{z}_0^2}}{i\bar{z}_x + \sqrt{1-\bar{z}_x^2}} \right)^{N4/\gamma} \quad (\text{Reflection coefficient at end of cochlea})$$

$$D(x, \omega) = c_1 \left(\frac{\omega}{\omega_r} \right)^{1/2} \left(\frac{i\omega/\omega_r}{\sqrt{1-\bar{z}_x^2}} \right) \left(\frac{\sqrt{1-\bar{z}_0^2}}{\sqrt{1-\bar{z}_x^2}} \right)^{1/2} \left(\frac{\Phi(x) + \frac{\Phi^2(L)}{\Phi(x)}}{1 + \Phi^2(L)} \right)$$

INTENTIONALLY LEFT BLANK.

Appendix B. Computer Programming and Source Code Applications*

*This appendix appears as an attachment to the PDF.

Approved for public release; distribution is unlimited.

List of Symbols, Abbreviations, and Acronyms

1-D	1-dimensional
AHAAH	Auditory Hazard Assessment Algorithm for Humans
ARU(s)	auditory risk units
ATF	acoustic test fixture
BM	basilar membrane
CTS	compound threshold shift
dB	decibels
dBp	decibels pressure
DNA	deoxyribonucleic acid
DRC	damage risk criterion
HPD(s)	hearing protection device(s)
HPM	Hearing Protection Module
MIL-STD	Military Standard
MIRE	microphone-in-real-ear
OC	organ of Corti
OV	occluded volume
PPL(s)	peak pressure level(s)
PTS	permanent threshold shift
Q	quality factor
REAT	real ear attenuation at threshold
S(s)	subject(s)
SD(s)	standard deviation(s)
SPL(s)	sound pressure level(s)
TS	threshold shift
TTS	temporary threshold shift
WKB	Wentzel–Kramers–Brillouin Approximation

1 DEFENSE TECHNICAL
(PDF) INFORMATION CTR
DTIC OCA

2 DIR ARL
(PDF) IMAL HRA
RECORDS MGMT
RDRL DCL
TECH LIB

1 GOVT PRINTG OFC
(PDF) A MALHOTRA

1 ARMY RSCH LAB – HRED
(PDF) RDRL HRB B
T DAVIS
BLDG 5400 RM C242
REDSTONE ARSENAL AL
35898-7290

8 ARMY RSCH LAB – HRED
(PDF) SFC PAUL RAY SMITH CTR
RDRL HRO COL H BUHL
RDRL HRF J CHEN
RDRL HRA I MARTINEZ
RDRL HRR R SOTTILARE
RDRL HRA C A RODRIGUEZ
RDRL HRA B G GOODWIN
RDRL HRA A C METEVIER
RDRL HRA D B PETTIT
12423 RESEARCH PARKWAY
ORLANDO FL 32826

1 USA ARMY G1
(PDF) DAPE HSI B KNAPP
300 ARMY PENTAGON
RM 2C489
WASHINGTON DC 20310-0300

1 USAF 711 HPW
(PDF) 711 HPW/RH K GEISS
2698 G ST BLDG 190
WRIGHT PATTERSON AFB OH
45433-7604

1 USN ONR
(PDF) ONR CODE 341 J TANGNEY
875 N RANDOLPH STREET
BLDG 87
ARLINGTON VA 22203-1986

1 USA NSRDEC
(PDF) RDNS D D TAMILIO
10 GENERAL GREENE AVE
NATICK MA 01760-2642

1 OSD OUSD ATL
(PDF) HPT&B B PETRO
4800 MARK CENTER DRIVE
SUITE 17E08
ALEXANDRIA VA 22350

ABERDEEN PROVING GROUND

11 DIR USARL
(PDF) RDRL HR
J LOCKETT
P FRANASZCZUK
K MCDOWELL
K OIE
RDRL HRB
D HEADLEY
RDRL HRB C
J GRYNOVICKI
RDRL HRB D
C PAULILLO
RDRL HRF A
A DECOSTANZA
RDRL HRF B
A EVANS
RDRL HRF C
J GASTON
RDRL HRF D
A MARATHE

INTENTIONALLY LEFT BLANK.